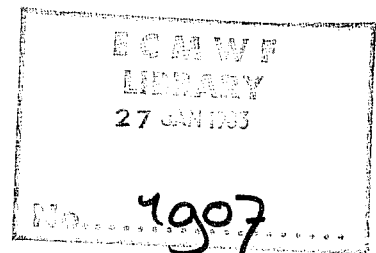


TECHNICAL REPORT No. 34

THE IMPACT OF CLOUD TRACK WIND DATA ON GLOBAL ANALYSES AND MEDIUM RANGE FORECASTS

by

P. Kållberg¹, S. Uppala¹, N. Gustafsson² and J. Pailleux³



December 1982

1 ECMWF

2 Swedish Meteorological and Hydrological Institute, Norrköping, Sweden

3 Direction de la Météorologie, Paris, France

C O N T E N T S	PAGE
1. INTRODUCTION	1
2. THE ASSIMILATION PERIOD	4
3. DATA ASSIMILATION SYSTEM AND FORECAST MODEL	6
4. IMPACT ON ANALYSES	11
4.1 Statistical evaluation of analysis differences	11
4.2 Synoptic evaluation of analysis maps	31
4.3 Quality of satellite wind data and problems in the analysis of these data	38
5. IMPACT ON FORECASTS	42
5.1 General impact on forecast error statistics	42
5.2 Synoptic evaluation of forecast maps	48
6. A FORECAST EXPERIMENT WITH ANALYSES AS LATERAL BOUNDARY CONDITIONS IN THE TROPICS	52
7. SUMMARY AND CONCLUSIONS	54
REFERENCES	58

1. INTRODUCTION

The influence or the impact of a set of observations on an analysis-forecast system can be considered as a function of the differences between the analyses and the forecasts produced with and without these data. Since it is known that different operational and research forecasting systems do vary in their skill even if they have the same observational data available, most of these differences must be due to the design of analysis schemes and forecast models. An objective evaluation of the impact should thus be based on several data-assimilations with different analysis-forecast systems and in order to make general conclusions the assimilations should be done over several synoptically different periods. The experiment described in this report is carried out using the ECMWF data assimilation system. It is an intermittent data assimilation system using a multivariate optimum interpolation analysis, a non-linear normal mode initialization, and a high resolution forecast which produces a first estimate for the subsequent analysis. The observations are assimilated in 6 hour periods (Fig. 1.). The impact on the analysis depends not only on the observations and their quality but also on the internal constraints of the multivariate optimum interpolation scheme, such as the data selection procedures, quality of the first guess forecast as defined by its error characteristics and the quality of the observations as defined by the observation error statistics. The impact on the forecasts on the other hand is dependent on how much of the analysis impact is retained after the initialization and on how well the forecast model reacts to the analysis impact.

The present study on the impact of satellite cloud drift winds on medium range weather forecasts has been carried out as a part of ECMWF FGGE activities. Two parallel data assimilations (Fig. 2) one including (called WI) and one excluding (called WO) all cloud drift winds from geostationary satellites have been done for a two week period during the FGGE Special Observing Period I.

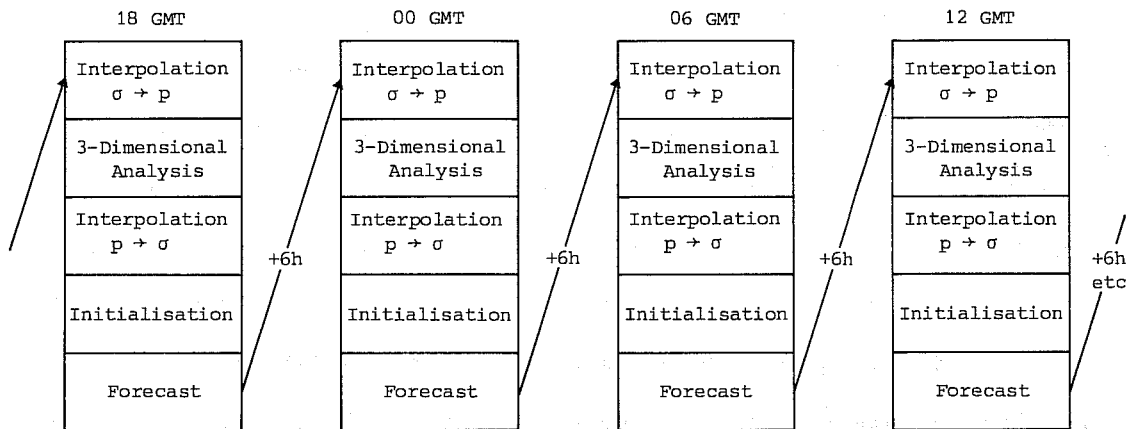


Fig. 1 Schematic outline of the data assimilation.

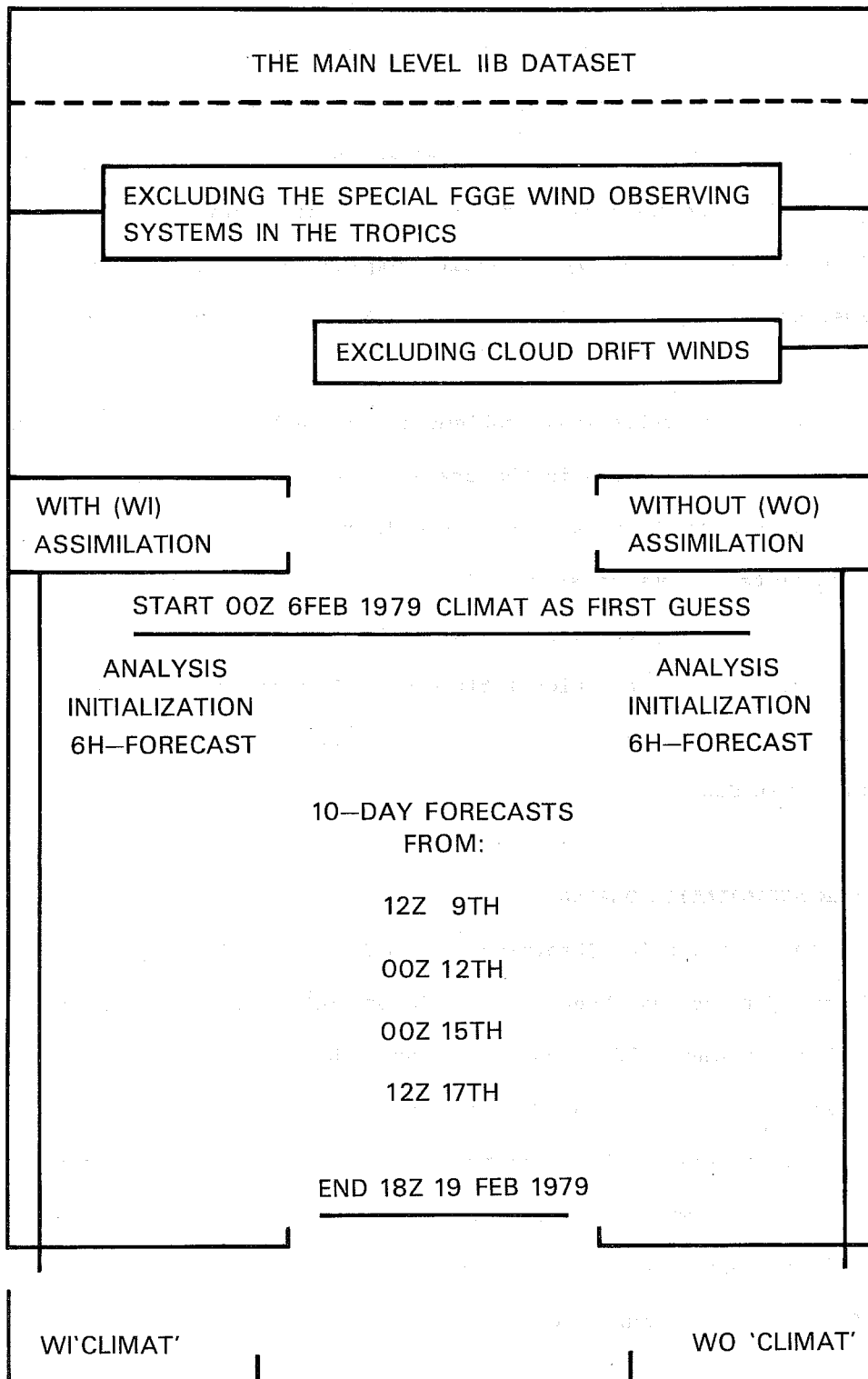


Fig. 2 Design of the experiment.

From the data-archives created during the assimilations and synoptic monitoring of the runs, verification statistics were produced, four forecasts were run and the averages of the assimilations were created. After a more detailed description of the assimilations in Sections 2 and 3 the impact on analyses is described in Section 4, as a statistical study of analysis differences (4.1), and by synoptic comparison of the WI and WO analyses against each other and against the ECMWF level IIIb analyses (4.2).

As a part of the evaluation, problems in the quality of the cloud drift wind data, as well as problems in the usage of such data in ECMWF assimilation scheme, were encountered and these are discussed in Sect. 4.3. The impact on forecasts is evaluated in Sect. 5 by verifying four forecasts both subjectively and objectively. In order to measure the tropical influences on a forecast in middle and high latitudes, a forecast was run in which analyzed fields replaced the forecast within an equatorial belt. The results are discussed in Section 6.

2. THE ASSIMILATION PERIOD

During the FGGE Special Observing Period I, from 5 January 1979 to 5 March 1979, two periods have been selected by JSC/WGNE for numerical experiments, 6-30 January and 8-22 February. Both these periods contain several interesting situations in the northern hemisphere, dominated by north Atlantic blockings and blocking breakdowns. For the present experiment the February period, with a better data coverage, was chosen. An example of the data amount during this period is given in Table 1. From the Level I Ib data the following data sources were excluded:

Table 1. The FGGE level II-b data amount 9 Feb 1979.

		00	06	12	18	GMT
Rawinsonde data (excluded)		780	75	767	146	
Pilot wind data		512	435	578	355	
TWOS NAVAIID (all excluded)		9	7	10	9	
Dropwindsonde (all excluded)		6	18	12	18	
Constant level balloon (all excluded)		53	53	49	50	
Aircraft data (ASDAR)		63	47	32	58	
	(AIDS)	527	478	395	602	
	(AIREP)	864	1079	658	866	
Surface	SYNOP	2323	2412	2566	2380	
	SHIP fixed	23	26	26	28	
	mobile	1132	1091	1096	1017	
Satellite sounding data	cloudy	487	483	564	510	
	partly cloudy	283	274	249	258	
	clear	1238	1312	1253	1262	
Satellite cloud drift winds						
NESS	high level	157	-	150	160	
	low level	46	-	268	367	
WISCONSIN	high level	598	-	647	541	
	low level	116	-	349	989	
LMD	high level	-	133	-	-	
	low level	-	334	-	-	
METEOSAT	high level	372	-	292	-	
	low level	88	-	139	-	
HIMAWARI	high level	193	-	184	-	
	low level	306	-	102	-	
High level winds/6 hour		1320	133	1273	701	
Low level winds/6 hour		556	334	858	1356	
Drifting buoy data		363	444	352	418	

- (a) TWOS Radar sounding data
- (b) TWOS NAVAID sounding data
- (c) Aircraft dropwindsonde data
- (d) Constant-level balloon data
- (e) FGGE Special Island sounding data

The reason for excluding these data was that 1) being special observations they are not (yet) available in the Global Telecommunication System (GTS) and 2) they can be used as independent verifying observations in the tropics. The geographical distribution of the cloud drift winds in Table 1 is given in Fig. 3 for 06 and 12GMT.

3. DATA ASSIMILATION SYSTEM AND FORECAST MODEL

The ECMWF data assimilation system (Bengtsson et al 1982) was used for the two analysis series. It is an intermittent, four-dimensional data assimilation system consisting of a multi-variate optimum interpolation, a non-linear normal mode initialization and a first guess forecast using the operational ECMWF forecast model. Analyses were prepared for every 6th hour, using all data within the 6 hour time interval centred at the analysis times. A summary of the main features of the system is given in Appendix 1, and in this section we will only describe some features of relevance to the present experiment.

A major source of uncertainty in the cloud drift wind data is the assigned cloud heights. These are normally determined from the observed cloud top radiation temperatures, which are converted to pressure levels using some assumed temperature-pressure profile, either climatology or a standard atmosphere. In four-dimensional data assimilation systems, where a first guess, i.e. forecast temperature-pressure profile is available, it is possible to check the reported cloud levels against the forecast and possibly modify the levels if the forecast profile deviates from the one used for the

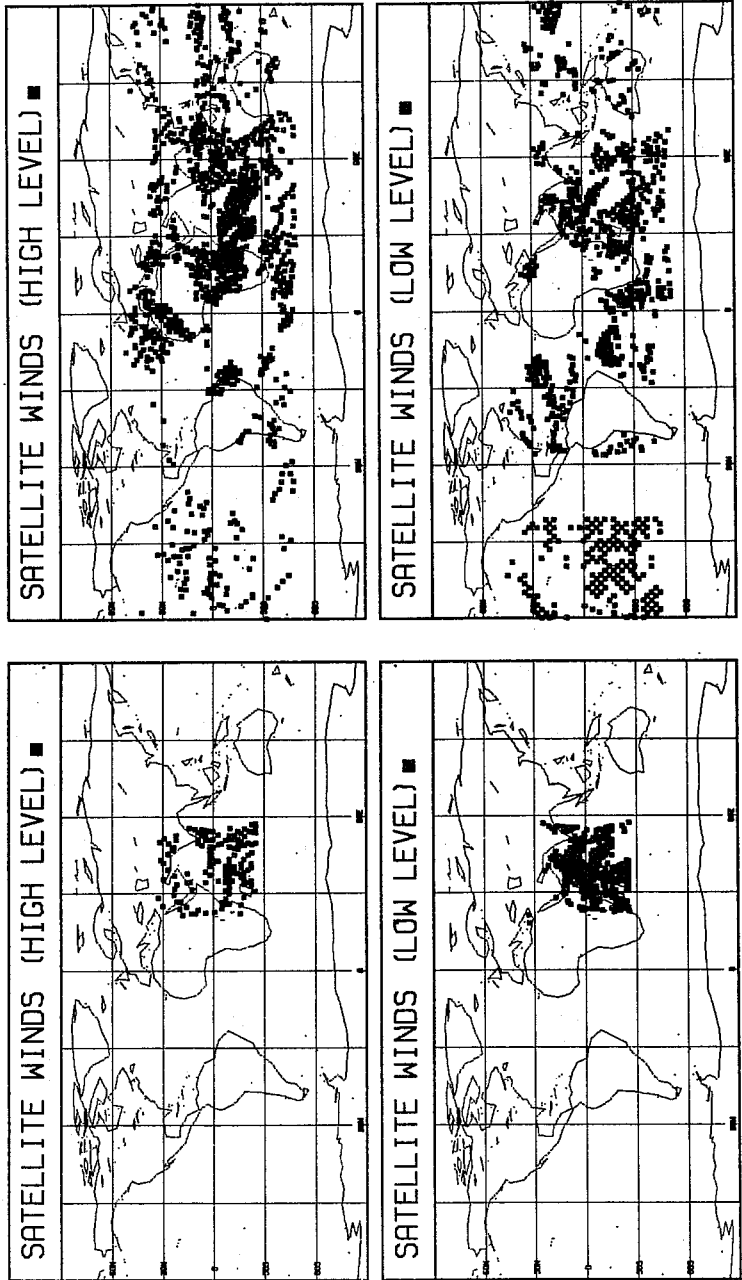


Fig. 3 Distribution of cloud track winds. 9 Feb. 1979, 06 GMT (left) and 12 GMT (right).

cloud wind derivations. A procedure to check and possibly modify the reported cloud wind data was applied above 600 mb during the ECMWF FGGE Level III-b production and in the present experiments the same height modification procedure was used.

In the ECMWF analysis scheme the observational data are subject to a three step quality control; a comparison with the first guess forecast, a comparison with neighbouring data and a comparison with a preliminary analysis interpolation to the position of, but excluding, the observational data to be checked. The acceptance/rejection criteria are based upon estimates of the error and error covariances of the first guess forecast as well as the observations. The first guess error is estimated using a vertical average of the analysis error which itself is a by-product of the optimum interpolation procedure. For details, see Lorenc (1981). Lacking a detailed evaluation of the statistical properties of the ECMWF model forecast errors, the covariances used were those given by Hollett (1975) and extended to the ECMWF model resolution. Those errors statistics are however not ideal; indeed they did cause some adverse effect in the analyses, which will be described below in Section 4.

The observation error estimates used in the experiment are listed in Table 2. In addition, during FGGE, certain observation systems, such as TWOS-Navaid and the tropical constant level balloons, provided their own error estimates. The numerical values in Table 2 were compiled from the following sources: Hollet (1975), Schlatter (1981) and unpublished information from NMC, Washington.

In the present experiments the analysis increments, not the full fields, were interpolated from the analysis pressure levels to the initialization/forecast σ -levels. This method, which was not used during the level III-b production,

TABLE 2 Observational errors for different observing systems.

Level (mb)	Temperature ($^{\circ}\text{C}$)				Wind (m s^{-1})				
	TIROS-N		Radiosonde		Radiosonde		Cloud-drift wind		
	Clear/ partly cloudy	Microwave	ASDAR AIDS	pilot	WISCONSIN	NESS	ESA	LMD	HIMAWARI
10	4.5	2.8	2.8	2.8	6	8	8	8	13
20	3.8	2.6	2.7	2.7	6	8	8	8	13
30	3.2	2.5	2.6	2.6	6	8	8	8	13
50	2.7	2.4	2.5	2.5	6	8	8	8	13
70	2.3	2.2	1.4	1.4	6	8	8	8	13
100	2.1	2.0	1.6	1.6	6	8	8	8	13
150	2.1	2.0	1.7	1.7	6	8	8	8	13
200	2.0	1.9	1.8	1.8	6	8	8	8	13
250	1.8	1.9	1.9	1.9	6	8	8	8	13
300	1.6	1.8	2.0	2.0	6	8	8	8	13
400	1.5	1.8	2.2	2.2	5	7	8	8	10
500	1.2	1.7	2.2	2.2	4	7	8	8	10
700	1.1	1.8	2.5	2.5	3	5	8	8	6
850	1.1	2.0	3.9	3.9	2	4	7	7	6
1000	-	-	-	-	2	4	7	7	6

Sea surface pressure: SYNOP/SHIP 1.0 mb; buoy 2.0 mb; COLBA/DROPWINDSONDE/TWOS-NAVAID observation errors are calculated from the level II-b quality information. Temperatures given as layer means.

guarantees that the first guess forecast is carried unaltered through the analysis in data void areas. Furthermore, since the vertical resolution in the boundary layer is much higher in the σ -level system than in the pressure level system, interpolation of the analysis increments results in less destruction of the boundary layer, compared to the full field interpolation.

All forecasts start from initialized analyses. At middle- and high latitudes the non-linear normal mode initialization very effectively eliminates unwanted gravity waves while the synoptically important divergence patterns are retained. In the tropics on the other hand non-linear normal mode initialization schemes do not perform as well, in that large scale divergence is suppressed. This will be demonstrated in Section 4.1 below. Important synoptic scale divergence systems in the tropics may thus be severely damaged by the initialization.

The good coverage of tropical wind observations during FGGE, made it possible to observe synoptic scale divergence systems with good accuracy. These systems were also analysed reasonably well by the optimum interpolation in data dense areas; but after the initialization they were markedly suppressed. This would mean that the impact of the tropical cloud wind data upon tropical forecasts may be underestimated by the present experiments.

Experience at ECMWF has shown that the behaviour of the forecast model in tropical areas is highly sensitive to the convection parameterization scheme. In the present experiments the ECMWF operational model's Kuo scheme formulation was used. There are indications that this formulation is not ideal and when examining the results in the tropics this should be remembered.

4. IMPACT ON ANALYSES

The two sets of analyses were evaluated statistically and synoptically. The statistical evaluation reveals some systematic differences between the two assimilations, while the synoptic evaluation explores typical differences in more detail.

4.1 Statistical evaluation of analysis differences

Systematic differences between the two assimilations were studied by calculating the root mean square (rms) difference and mean difference between the two sets of analyses for both wind and geopotential and at each analysis time for the 9 verification areas shown in Fig. 4. The time evolution of the wind rms difference, for a few selected areas, is shown in Fig. 5. There is some variability from analysis to analysis, mainly due to varying synoptic situations and varying cloud wind data distributions. In addition to the analysis to analysis variance, there is however also a tendency of increasing rms differences throughout the period. This is due to the gradual assimilation of more and more cloudwind data in the WI analyses, causing the windfields to develop differently also in data void areas through the 4-dimensional coupling with the forecast model.

Time averages of the rms differences for a few selected analysis parameters are shown in Table 3 for the different areas.

The largest height differences are found in the subtropical areas, particularly in the southern hemisphere. The difference over the small northern subtropic Atlantic area is also large. These areas contain very few radiosonde stations, thus the massfields are analyzed mainly from SATEM temperature profiles, and single level wind observations, the latter through the wind-mass coupling in the multivariate optimum interpolation. This coupling is larger in the subtropical areas (poleward of 15° latitude) than closer to the equator, hence the cloud wind data have a larger height impact

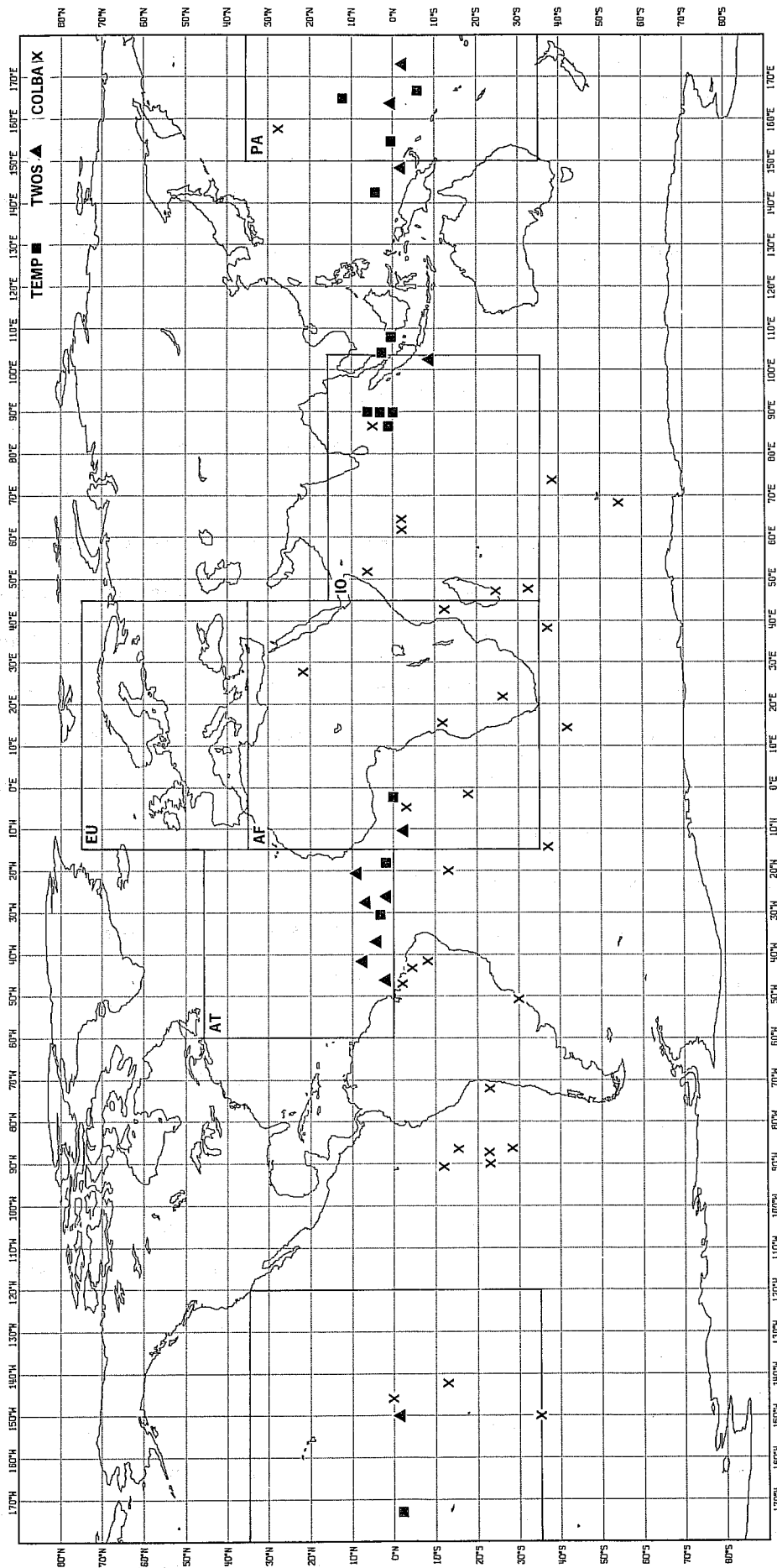


Fig. 4 Verification areas. Positions of verifying radiosonde data from TWOS and special islands.

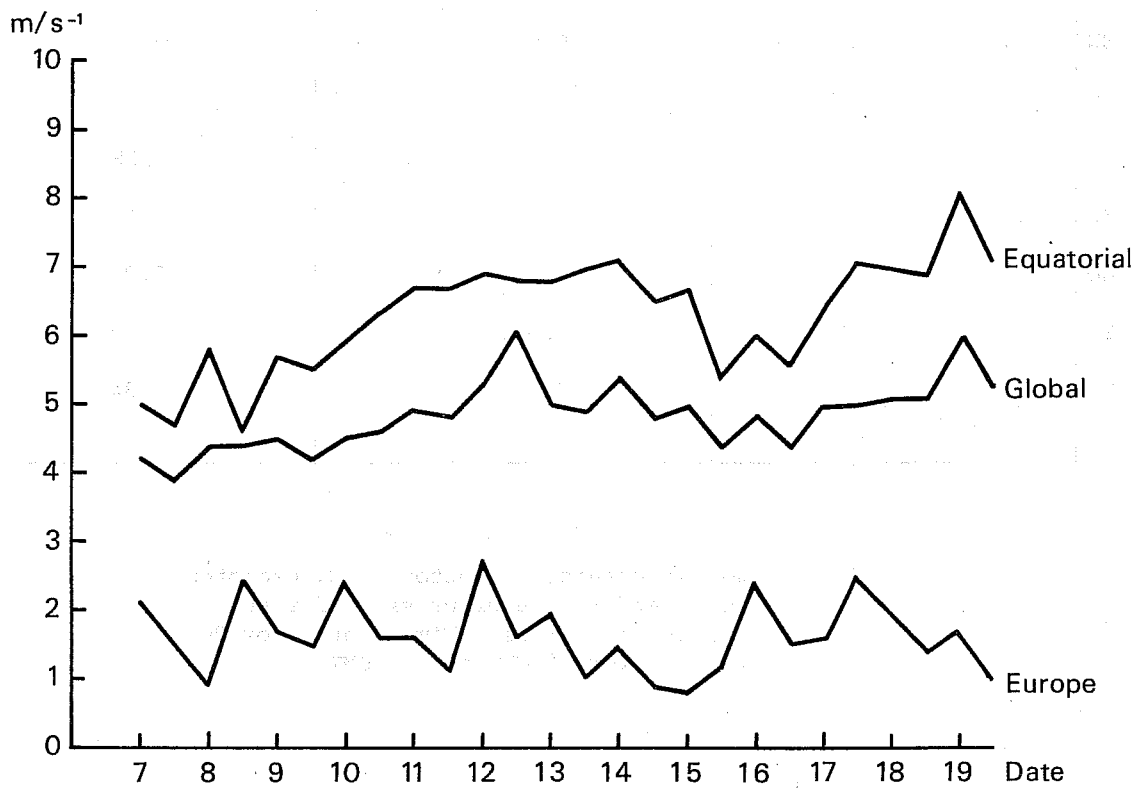


Fig. 5 Time evolution of 200 mb vector wind rms difference between WI and WO for 3 areas.

	<u>Wind Vector</u> (ms ⁻¹)		<u>Geopotential Height</u> (gpm)	<u>Sea-level Pressure</u> (mb)
	200mb	850mb	500mb	
GL	4.8	2.0	7.7	0.57
EQ	6.3	2.7	4.9	0.33
SN	4.3	1.7	5.0	0.29
SS	5.9	2.3	7.5	0.44
AF	5.1	1.4	4.7	0.28
EU	1.6	0.5	2.1	0.13
AO	4.7	2.1	7.6	0.28
IO	8.4	2.8	7.3	0.49
PO	5.0	2.9	5.9	0.34

TABLE 3 Rms differences of vector wind, Geopotential Height and Sea level pressure for the 9 verification areas. Time average of 26 analyses for 00 GMT and 12 GMT.

in the subtropics, in spite of the larger wind impact in the deep tropics (Table 3).

In middle and high latitude areas, such as Europe, the cloudwind impact on the height analysis is negligible. The impact from cloud wind data on mean sea level pressure analyses is always very small, possibly with an exception for middle latitudes in the southern hemisphere, where some synoptic cyclones have somewhat different structures in the two analyses.

The mean impact on the wind analyses is shown in Figs. 6a and 6b, where the vertical distribution of the rms difference is plotted for some selected areas.

The largest differences are found at 200 mb in the tropical areas. Particularly large impact is found over the Indian Ocean at this level. The period selected for the experiment was characterized by large amplitude, transient motion systems in the upper troposphere in this part of the world where cloud drift winds were the only wind observations available over large areas.

At 850 mb the largest wind differences were found over the Pacific Ocean. This will be shown later to be due to bad representation of the trade winds in the south-eastern part of the ocean in the WO analyses. A comparison of the global and the equatorial wind rms profiles, Fig. 6b, shows a more pronounced bimodal impact in the equatorial area with one maximum difference in the profiles at 850 mb and another at 200 mb. In the deep tropics, the observed clouds are normally found either at the trade wind cumulus level (850 mb) or cirrus level (200 mb), while midtroposphere clouds (altocumulus) are found more frequently at higher latitudes. The dynamic coupling between these levels is also smaller in the equatorial areas. In high latitude

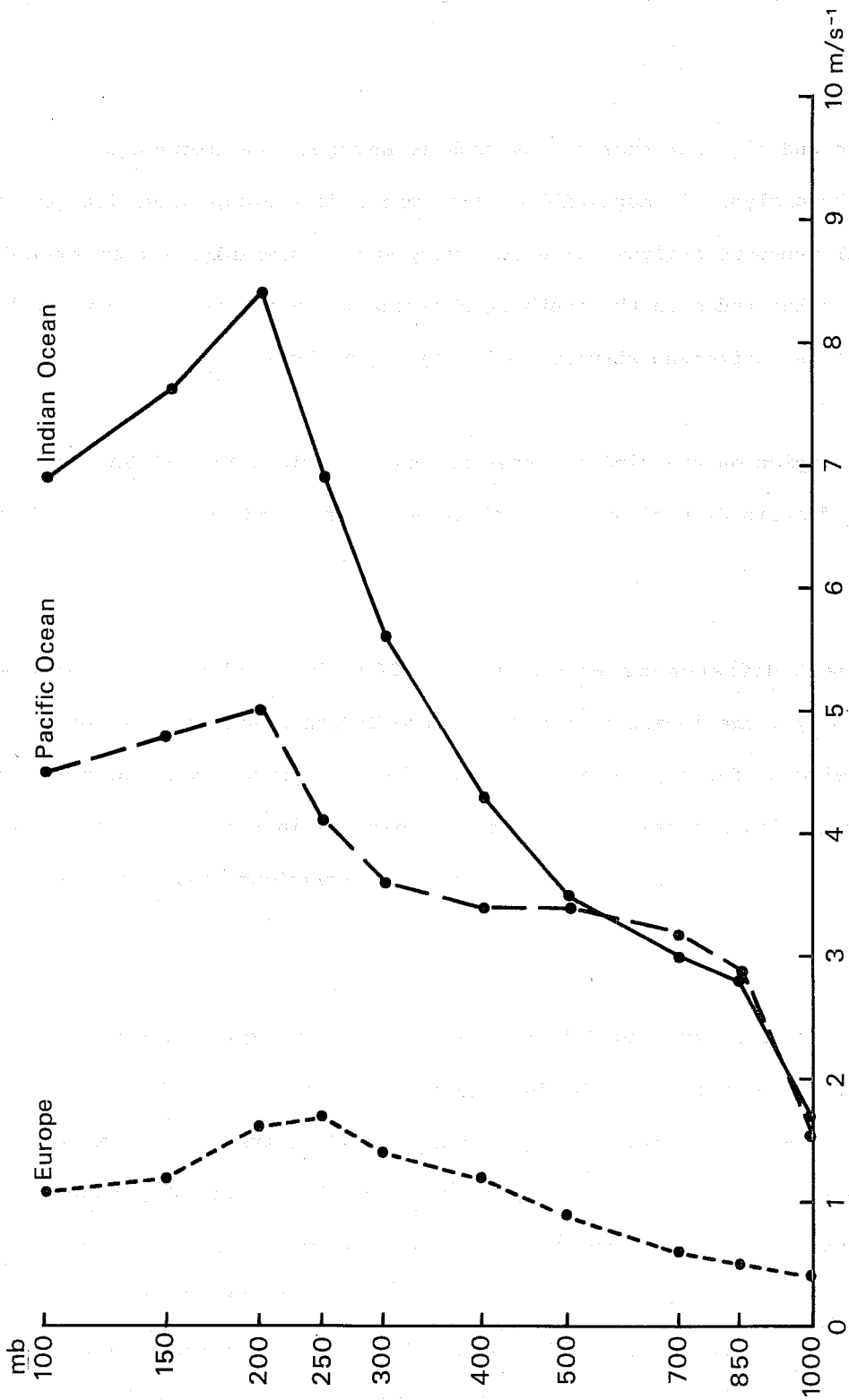


Fig. 6a Vector wind rms difference between WI and WO as function of height. 3 areas, EU, PO and IO. Europe, Pacific Ocean and Indian Ocean.

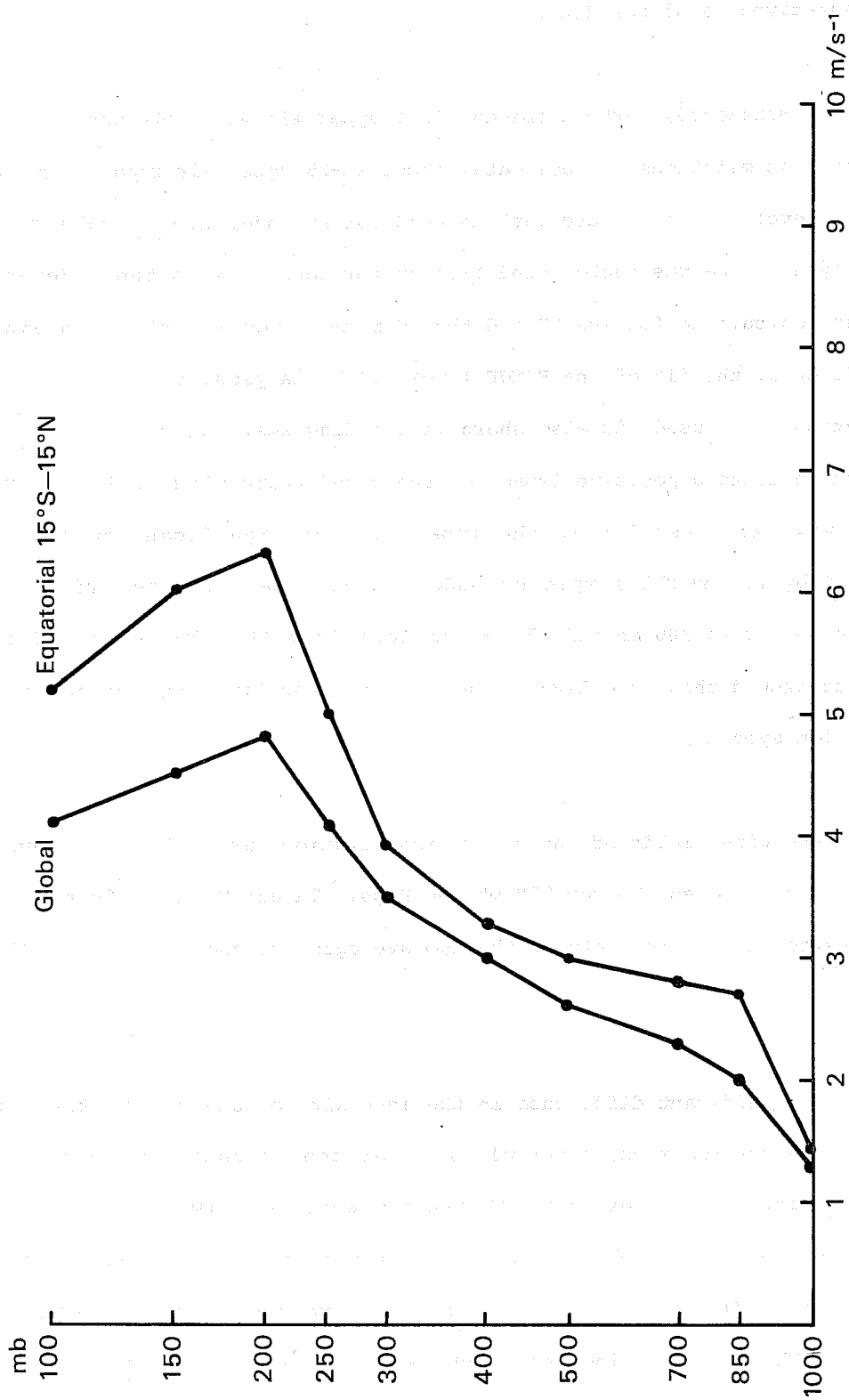


Fig. 6b As 6a, but global and equatorial.

areas, such as Europe, the wind impact is very small, below the representativeness of the data.

As already mentioned, certain special FGGE upper air wind data were excluded from both assimilations. These data, about 20-25 upper air reports and 40-45 constant level balloons, were instead used for an independent evaluation of the analyses. The rms vector wind fits of the analyses to the independent data were calculated for the WI and the WO runs, they are shown in Fig. 7. For reference, the fit of the ECMWF level III-b analyses, where the control observations were used, is also shown in the diagrams. With few exceptions the fits indicate a positive impact of the cloud track winds both at 200 mb and 850 mb. At other levels the impact is not significant enough to be verified by the small sample of independent data. The restriction of positive impact to 200 mb and 850 mb follows from the clustering of cloud wind data around these two levels, and the weak vertical coupling of tropical circulation systems.

Time average wind fields of the entire assimilation period from both runs are shown in Figs. 8a and 8b for 850 mb and Figs. 9a and 9b for 200 mb. Maps of the vector difference between the two averages are shown in Figs. 10 and 11.

There is a significant difference in the intensity of the 850 mb trade wind flow between the two runs, particularly over the southeastern part of the Pacific Ocean. The trades in the WI run are analyzed almost entirely from trade wind cumuli drift observations since there are very few other data in this region. Those few data from other sources do however confirm the analyses. The WO trade winds are much weaker, there is a large area with differences larger than 3 ms^{-1} and near the equator between 130° and 180°W the difference exceeds 5 ms^{-1} .

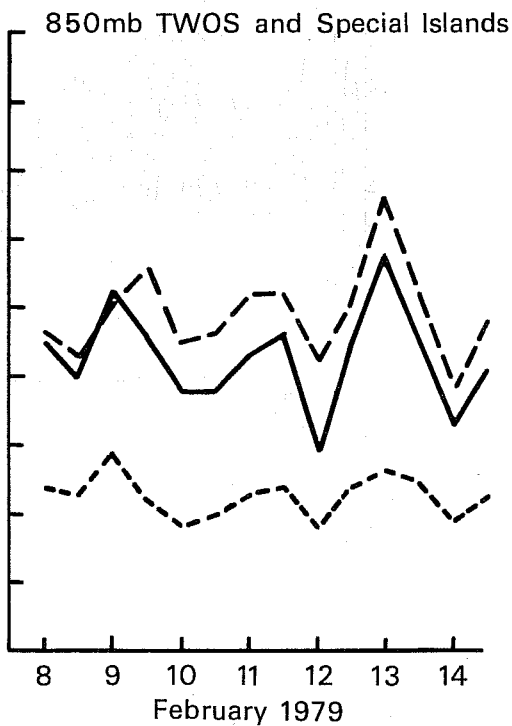
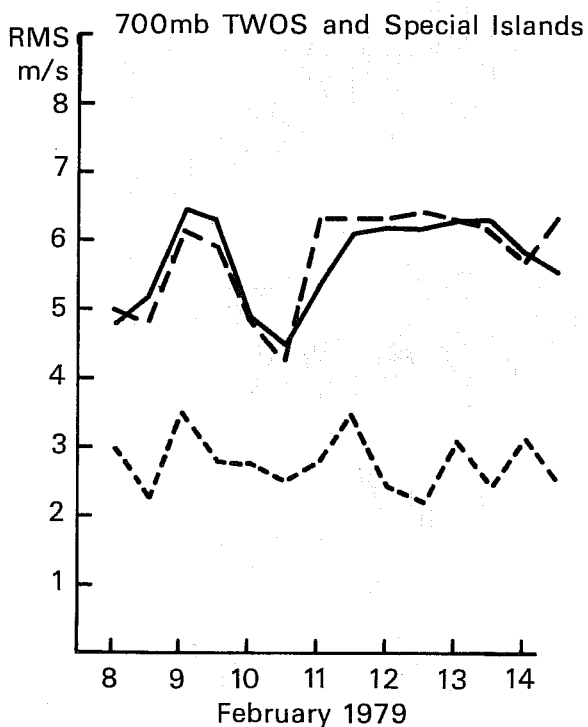
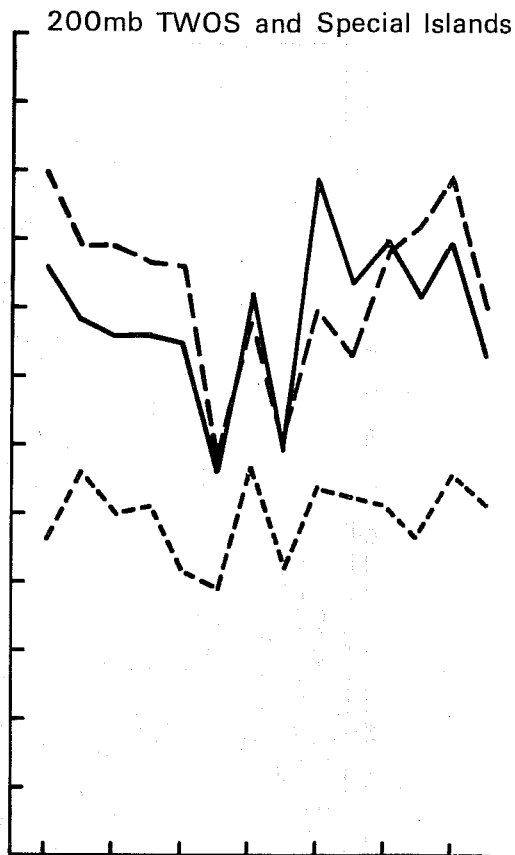
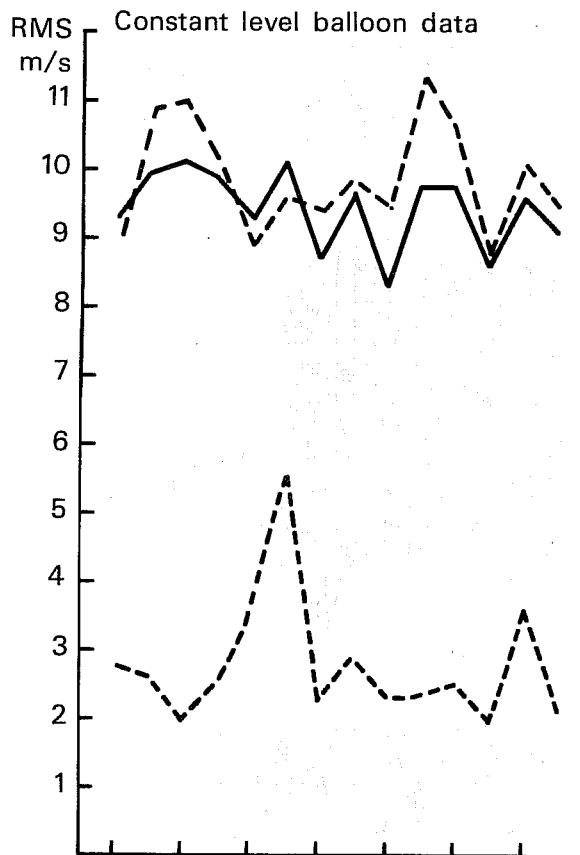


Fig. 7 RMS-fit of control data (not used) to analyses. With cloudwinds (full), without cloudwinds (dashed). Fit of these data to ECMWF III-b (where they were used) (dotted).

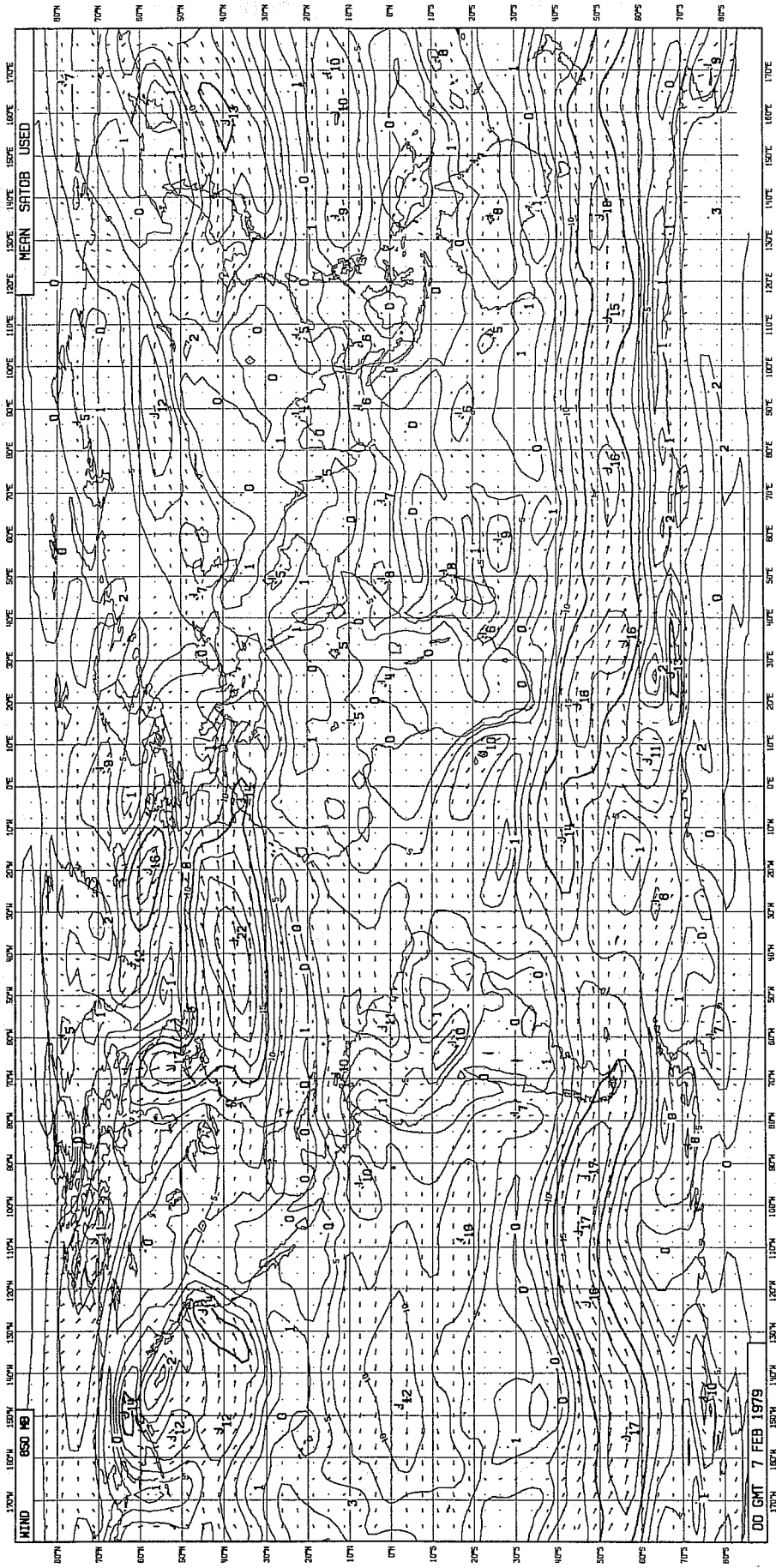


Fig. 8a Average wind analysis. 850 mb. With cloud winds (WI).

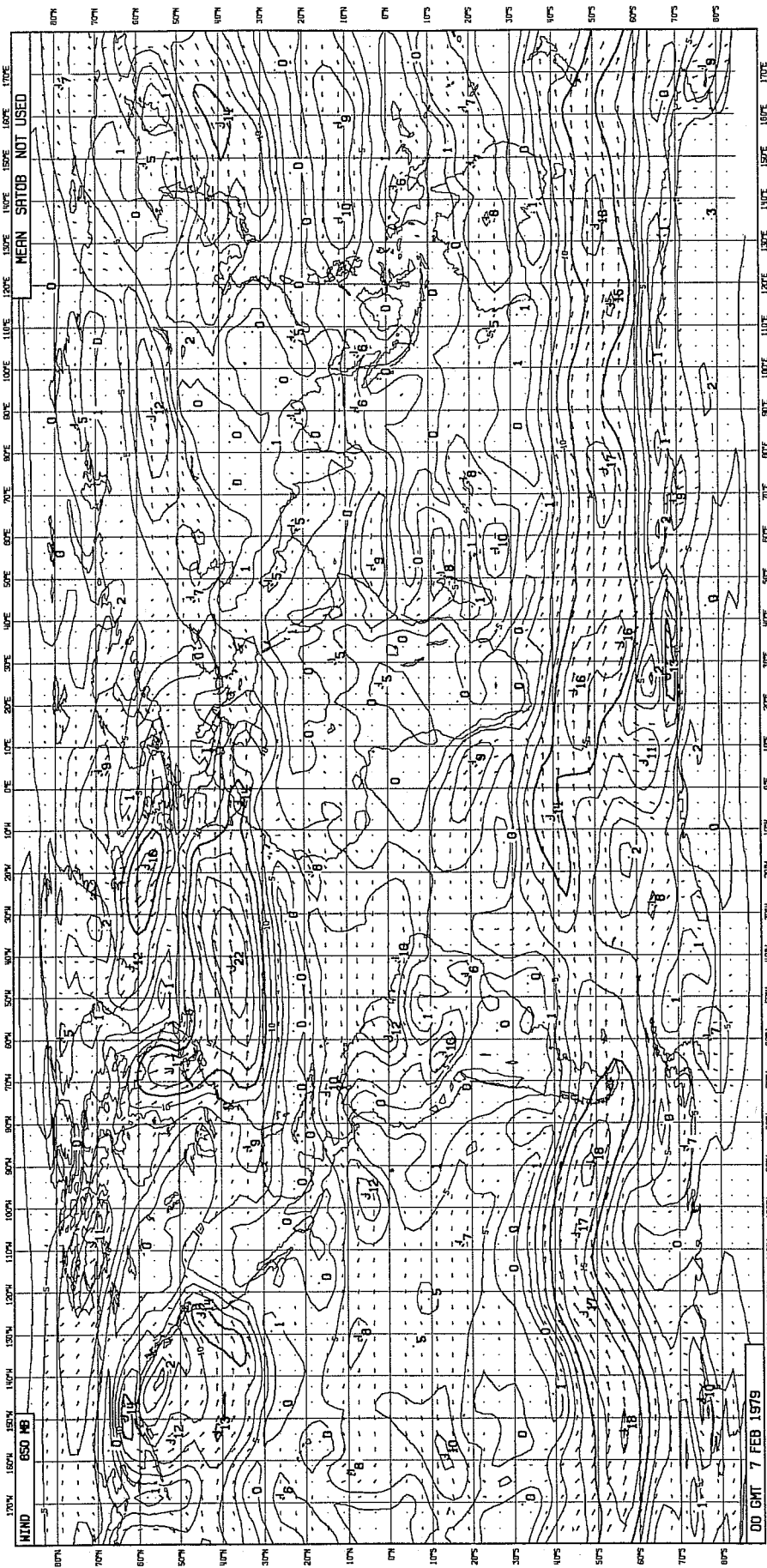


Fig. 8b As Fig. 8a, but without cloudwinds (WO).

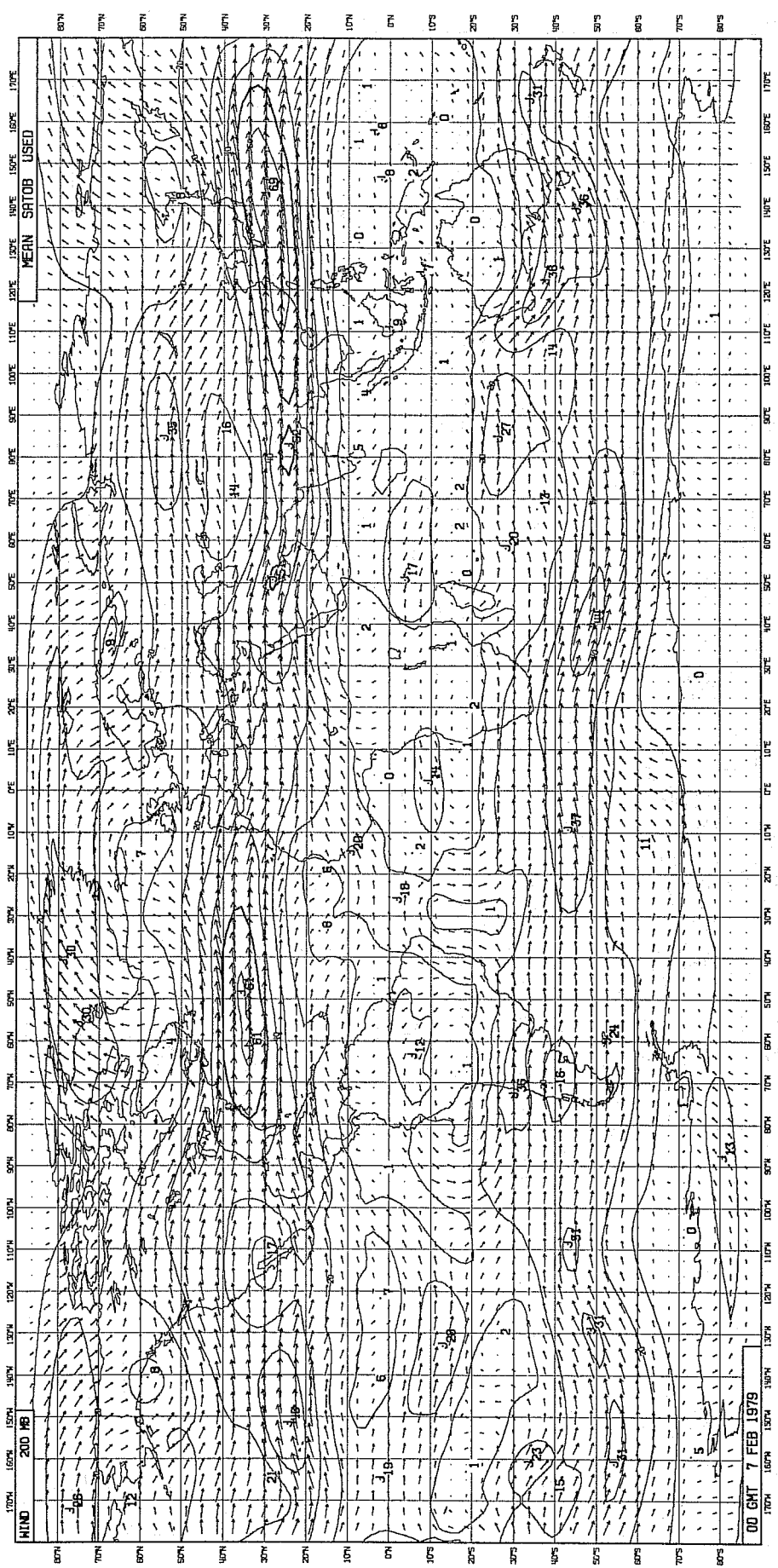


Fig. 9a Average wind analysis. 200 mb. With cloudwinds (WI).



Fig. 9b As Fig. 9a, but without cloudwinds (WO).

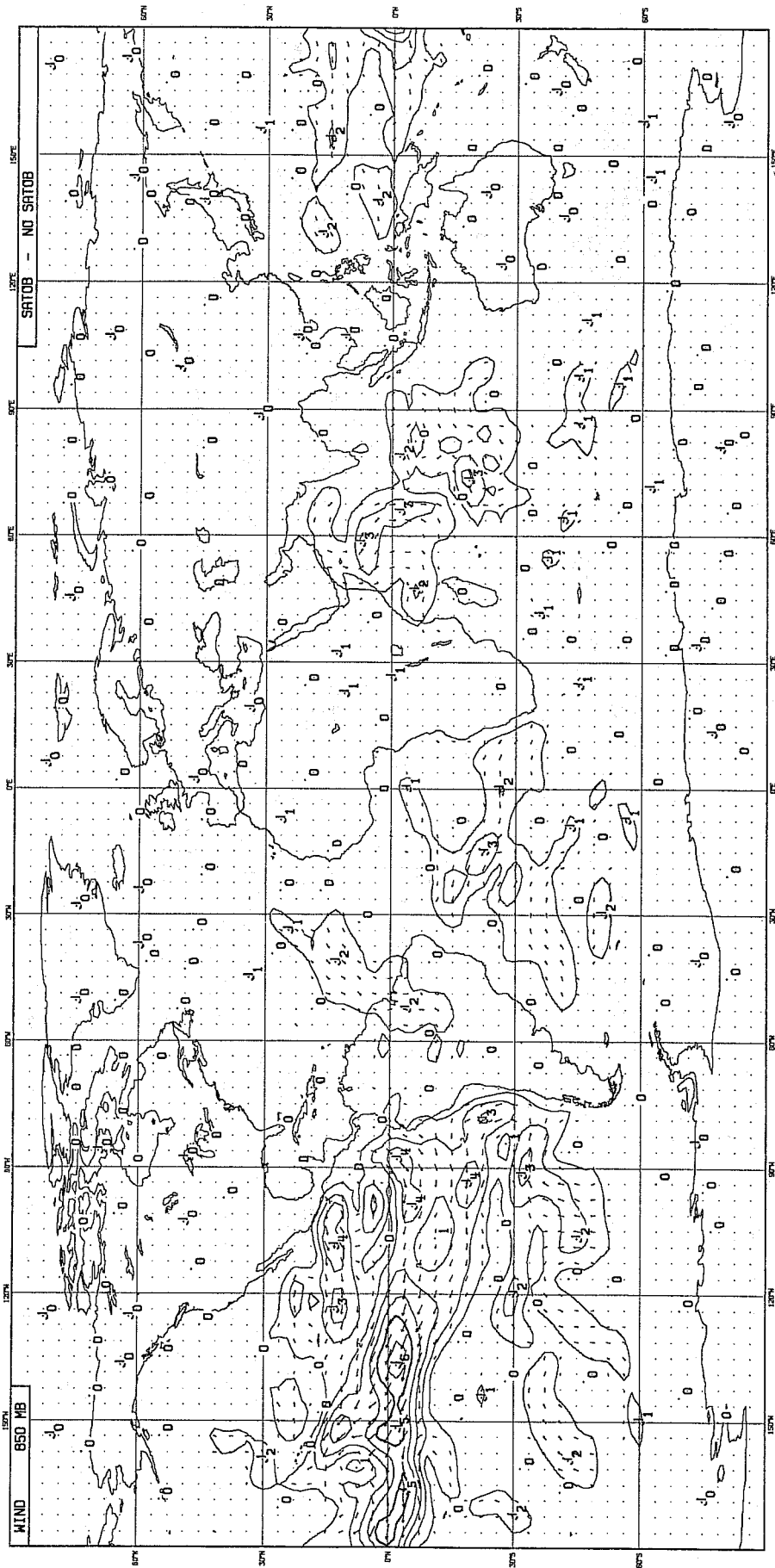


Fig. 10 Difference between averaged windfields (WI-WO). 850 mb.

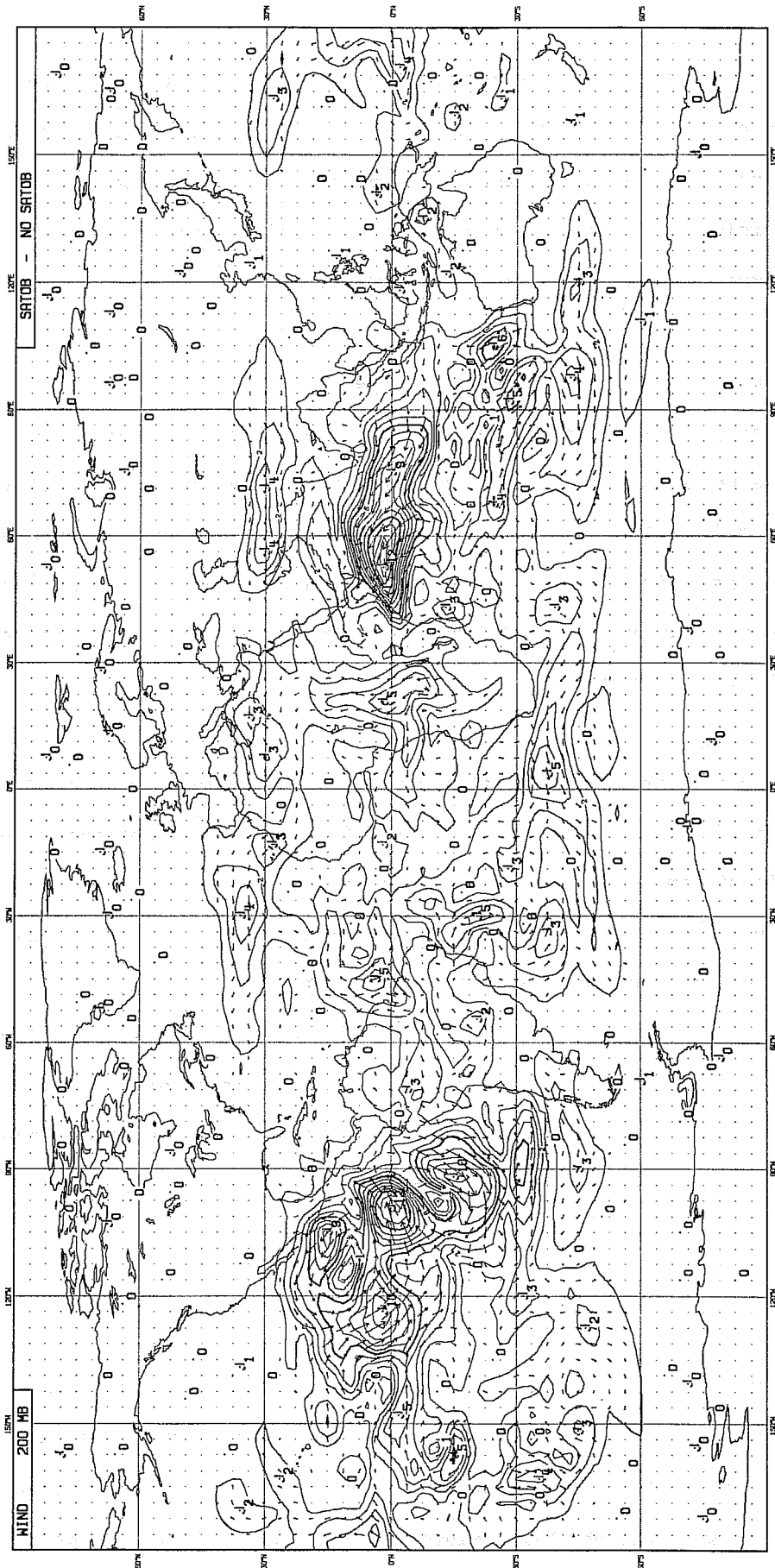


Fig. 11 As Fig. 10, but 200 mb.

The lack of trade winds in the WO run indicates an inability of the first guess forecast to generate trade winds of comparable intensity to that observed from the cumuli, at least at 850 mb. It is evident that in the present version of the assimilation scheme, the cloud wind data have a large positive impact on the analysis of the trades.

At 200 mb several areas of large differences between the two assimilations are found near the equator, the most striking at about 100°W and 60°E. These differences reflect synoptic systems with strong cross equatorial flows and with time scales of the order of a few days. Such events were observed during most periods of FGGE and in the otherwise data void areas in the eastern Pacific ocean and the Indian ocean, the cloud winds constituted the only available observations.

The importance of the cloud drift wind data for analysis of the tropical circulation is clearly demonstrated in Fig.12, which shows the zonal mean of the meridional wind component averaged for all 00GMT and 12GMT analyses in the two assimilations. In the first guess forecasts, upper panels, there is hardly any evidence of outflow in the upper part of the Hadley cell. This is due to the non-linear normal mode initialization, which, as mentioned in Sect.3, seriously suppresses divergence at low latitudes. The 6 hour forecast steps for the following first guesses, are not long enough to reestablish a realistic meridional cell. Indeed the residuals from the 5-mode cutoff in the initialization are still evident in the 6-hour forecasts.

The lower panels of Fig.12 show the corresponding mean meridional circulation from the uninitialized analyses. When cloud winds are used (left), a considerably more intense mean Hadley circulation has been obtained. The maximum outflow on the northern, winter, side of the cell increases from 1.5 ms^{-1} when cloud wind data are not used to 2.5 ms^{-1} when they are. There is

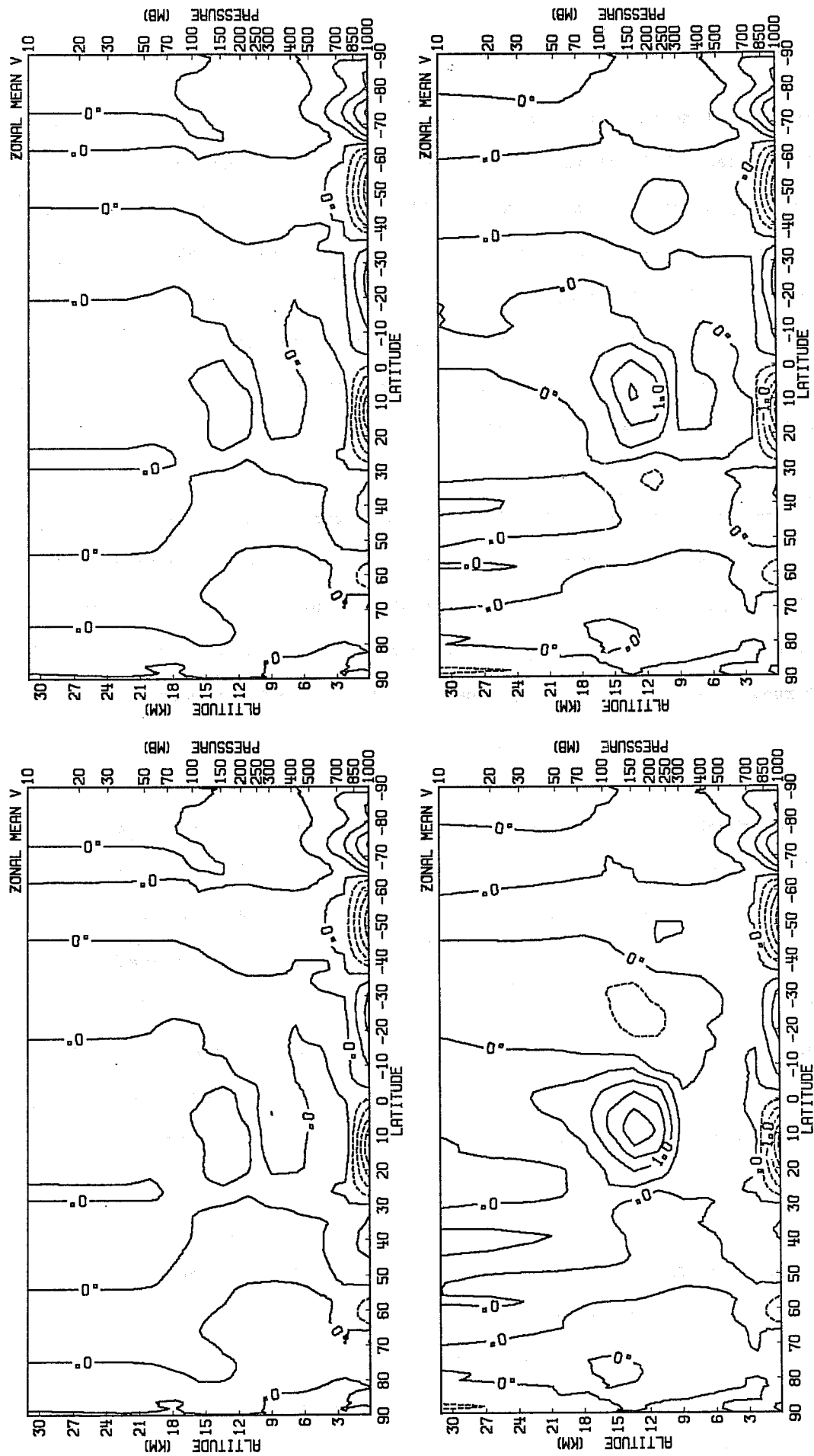


Fig. 12 Zonal average of mean meridional circulation. Left: with cloudwind data (WI), Right: without cloudwind data (WO), Top: first guess forecast, Bottom: analysis.

also a well defined outflow on the southern, summer, side of the ITCZ in the WI analyses, while it is almost absent in the WO analyses (right). The intensity of the zonally averaged Hadley cell in the WI run is only slightly weaker than the Dec-Feb average presented by Newell et al (1972). For comparison Fig.3.18 from their publication is copied in Fig.13. It can be concluded that cloud wind data are absolutely essential to analyse the upper troposphere mean circulation, at least within the context of global assimilation systems of the ECMWF type.

The importance of cloud wind data for upper tropospheric wind analyses at low latitudes is further emphasized in Fig.14, which shows the mean uninitialized velocity potential at 200 mb from the WI and the WO runs. Again there is a marked intensification of the divergence in the WI run when compared with the WO run. This is particularly true over the Indian Ocean where very few other data are available.

An important feature of the mean tropical circulation is the global scale circulation in the equatorial plane (Krishnamurti, 1979). The vertical circulation is very much dominated by a giant ascending cell centred over Melanesia in February. This feature is also much better analysed in the cloud wind assimilation, see Fig.14. The intensity of the divergent wind (normal to the contours of velocity potential) both in the zonal Walker cell centred at 150°E and the more Hadley like meridional cells over the Indian Ocean, central Africa and the Amazon region is more pronounced in the cloud wind mean.

A disturbing feature in the cloud wind analyses is the reduced intensity of the subtropical jets as compared with the assimilation without these data. This is most clearly seen over India, Iran, the Mediterranean area and the southern north Atlantic. (Fig.11). A comparison of individual analyses

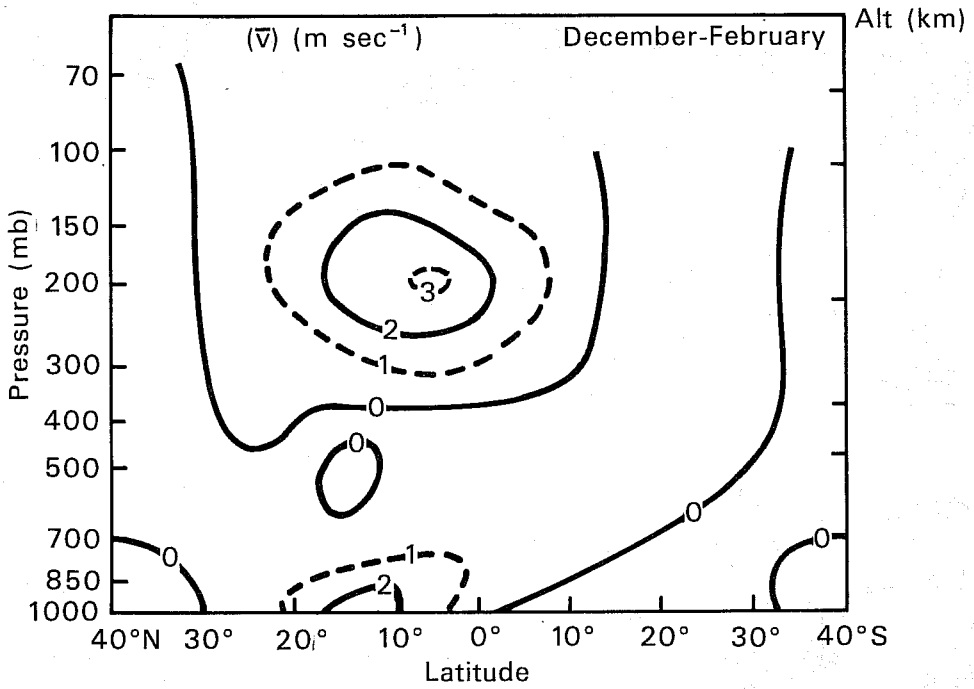


Fig. 13 Zonal average of mean meridional circulation.
Dec-Feb after Newell, et al.

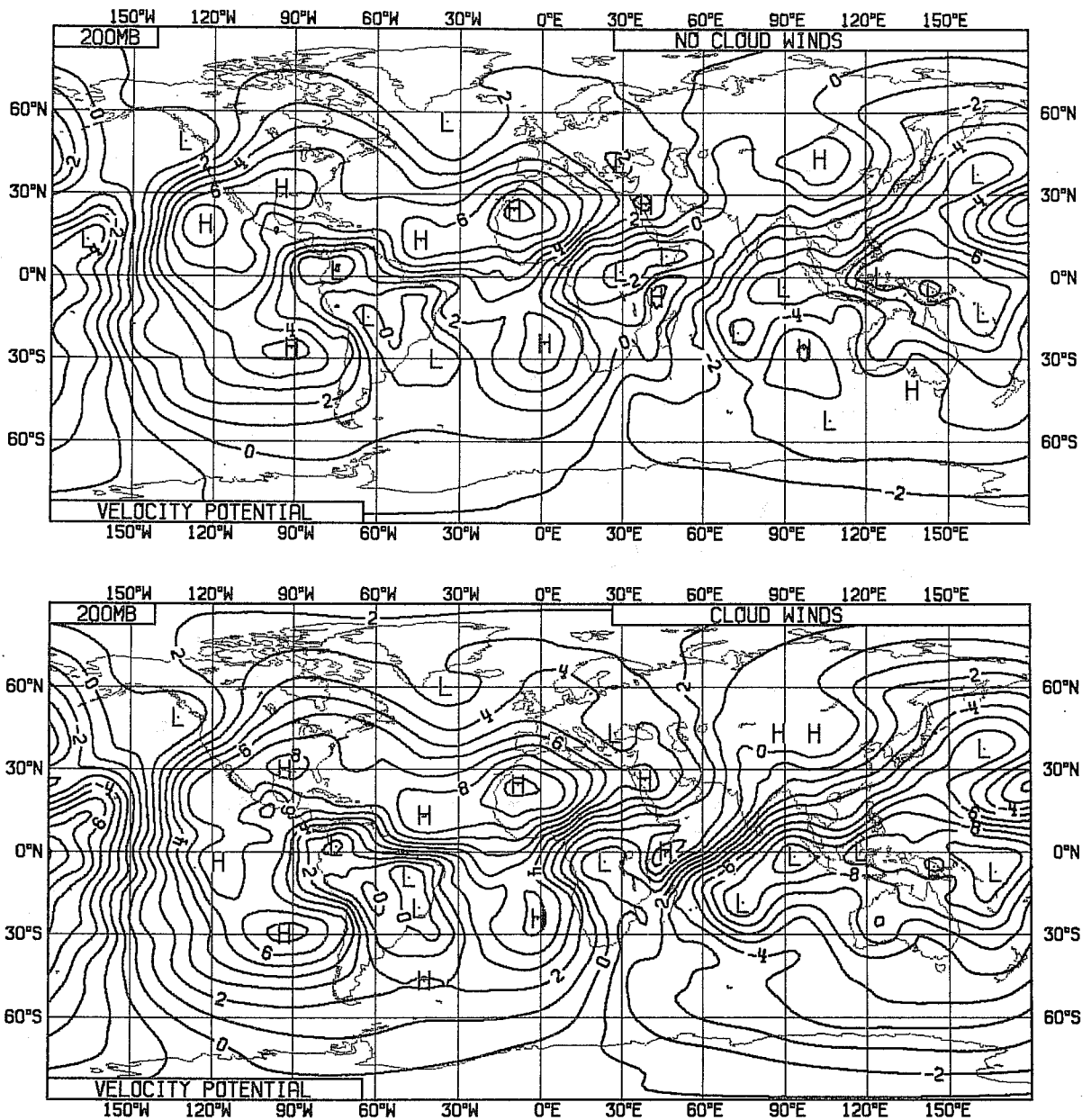


Fig. 14 Average velocity potential, 200 mb. No cloudwinds (top), cloudwinds (bottom)

revealed that the differences were caused by cloud drift winds with erroneously too low windspeeds compared to neighbouring radiosonde and aircraft data. Also the southern subtropical jetstream is weaker in the cloud wind analyses, although no colocated independent observations are available to prove that the clouds winds are in fact too weak. In Fig.15 the zonal mean of the total eddy kinetic energy is shown for the two assimilations. In the central parts of two subtropical jetstreams, the eddy kinetic energy is about 5% smaller in the cloud wind assimilation. The same applies to the zonal kinetic energy, (not shown). Over the equator, on the other hand, the eddy kinetic energy is larger in the cloud wind run, which is consistent with the comments to Fig.11. The problem of too weak cloud winds in the subtropical jets is further addressed in Sect.4.3 below.

4.2 Synoptic evaluation of analysis maps

At middle and high latitudes the mass- and wind field analyses from the two runs do not show significant differences at any of the days in the experiment. Large differences are however found in the tropical wind analyses, particularly in the upper troposphere. These differences are obviously most significant in areas with bad coverage of other data types.

A good example of the importance of cloud wind data for tropical wind analyses is shown in Fig.16. A large scale system of southeasterlies covers most of the area south of 5°N. Further north the winds turn more southerly, and eventually they merge with the southwesterlies of the northern subtropical jet. The wind field of the WO analysis on the other hand is broken up into several smaller circulation systems. Note in particular the complete reversal in the area 5°S 65°E, and the spurious double vortex structure around 90°E. The flow pattern in the WI analysis was verified by some independent FGGE ship data in the area.

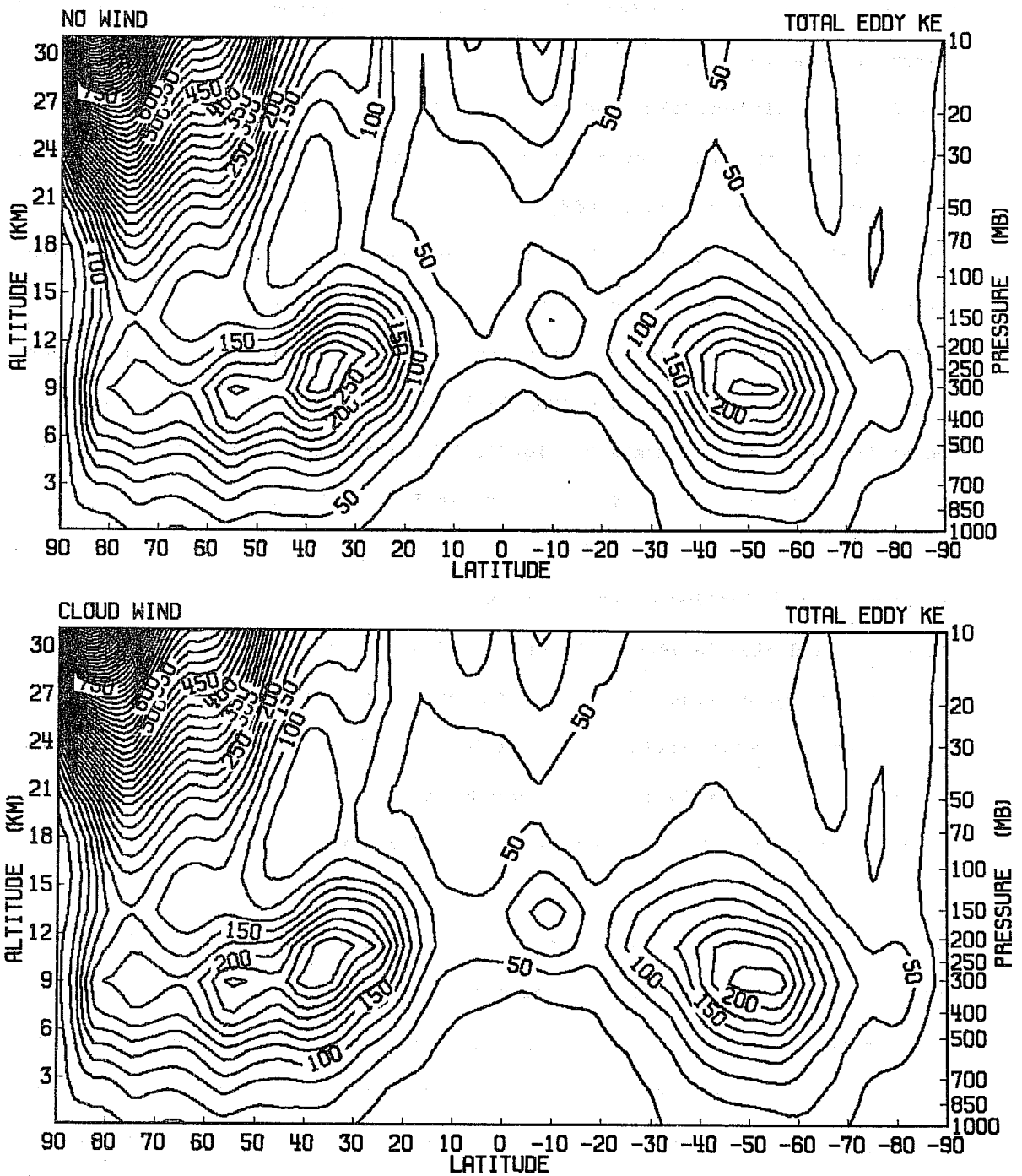


Fig. 15 Zonal average of total eddy kinetic energy. No cloudwinds (top), cloudwinds (bottom).

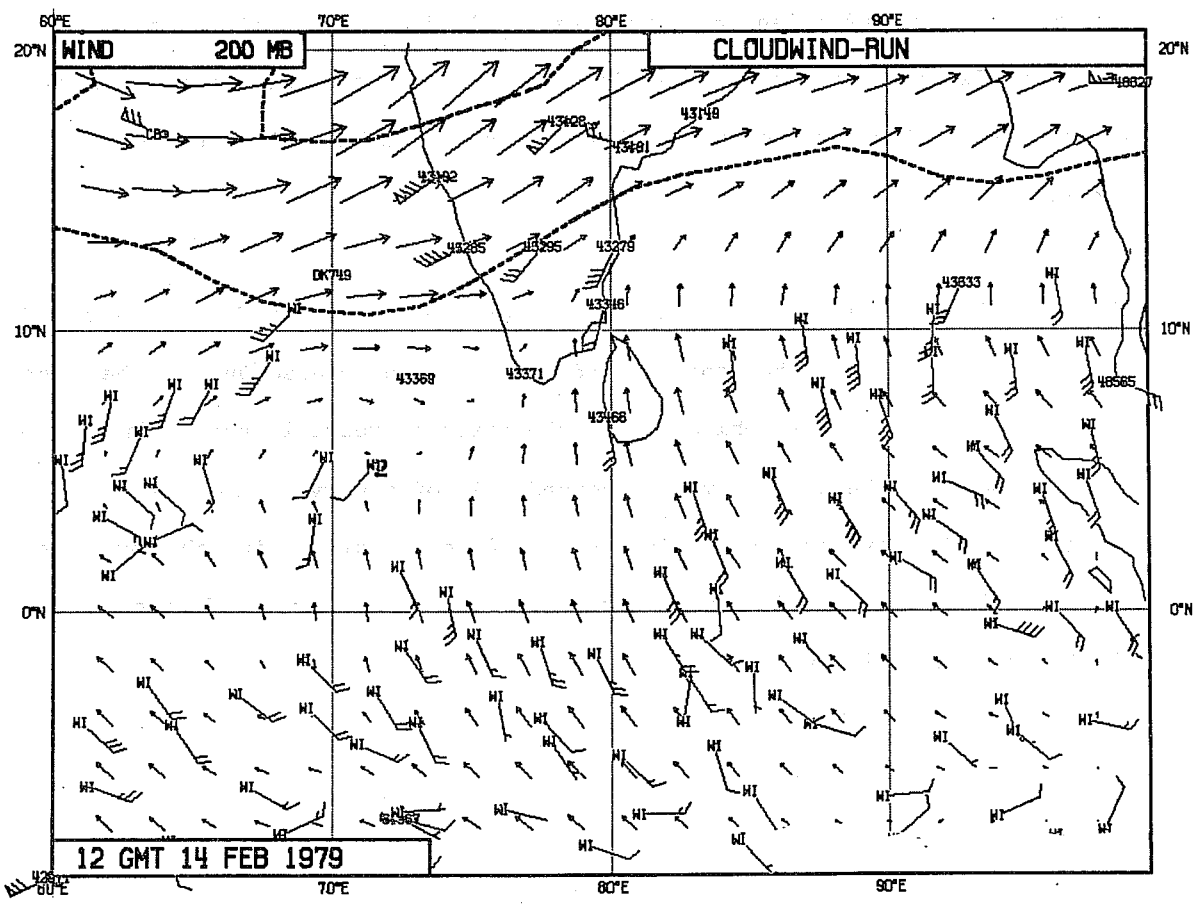
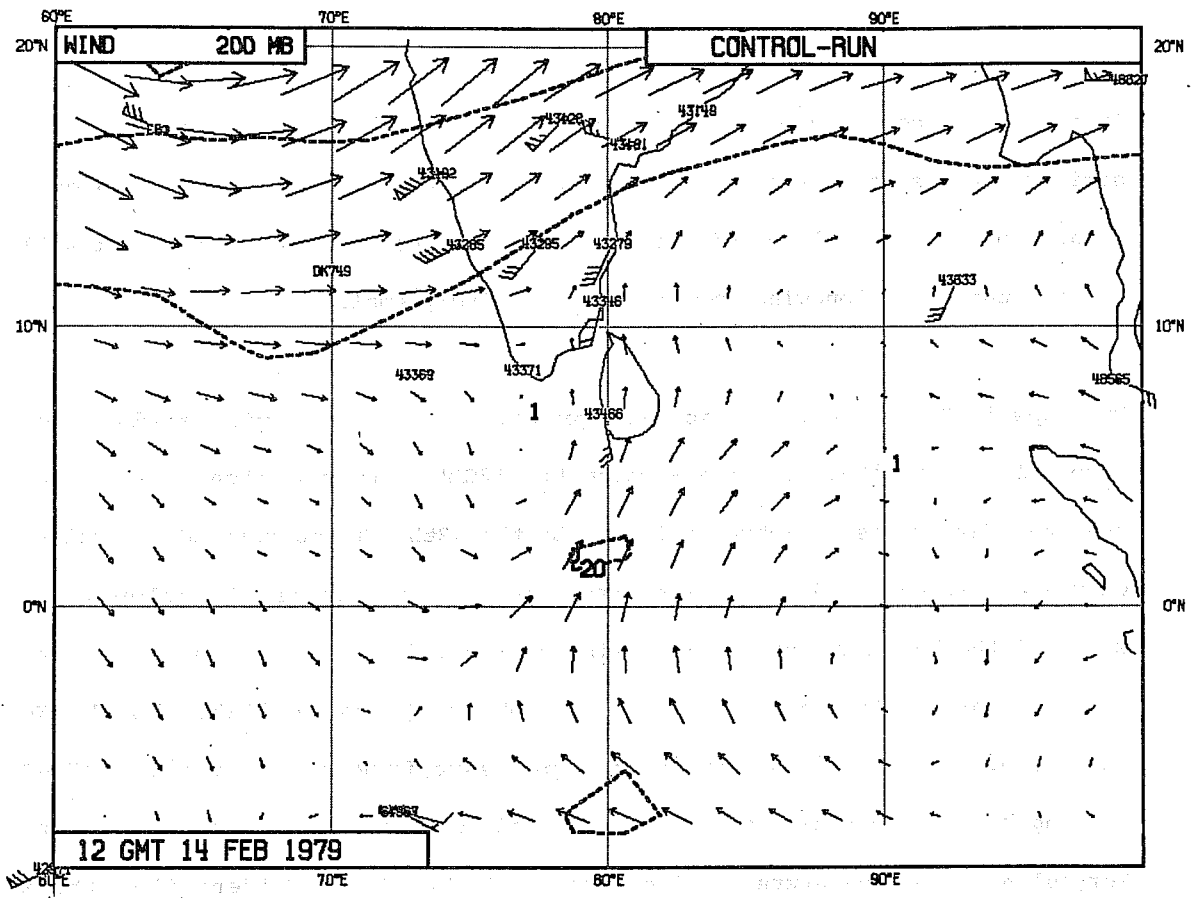


Fig. 16 Wind analysis 200 mb. 14 Feb 1979 12 GMT. No cloudwinds (top), cloudwinds (bottom).

In areas outside the equatorial zone ($15^{\circ}\text{S} - 15^{\circ}\text{N}$) the analyses are more similar. A case of a tropical cyclone, where one a priori might expect a great impact of the cloudwind data will be described in some detail. It will be seen that the cloudwind impact is surprisingly small.

The maps in Fig.17 show the surface pressure and 850 mb wind analyses of Tropical Cyclone 'Celine' on February 11, 12GMT. This cyclone was formed near the Mascarenes on February 3, and by the 12th, it had reached Kerguelen, whereafter it was gradually transformed into an extratropical cyclone. In spite of the large amount of cloud wind data available to WI assimilation, the two analyses look quite similar. The observations available to the WO run, were: surface winds and surface pressure from ships, and some FGGE drifting buoys; upper air data from radiosonde stations in the Mascarenes and Kerguelen; and temperature profiles from TIROS-N. It is evident that these observations are sufficient to give a realistic description of the cyclone in the four-dimensional data assimilation. Also the three-dimensional thermodynamic structures of the cyclone are very similar in the two runs, see Fig.18.

The WO cyclone is in fact the more intense of the two, with a warmer and drier core and stronger tangential winds. This is of course due to the less amount of upper air data, which allows the forecast model in the assimilation cycle to develop the cyclone more independently of observations. In the WI assimilation the cyclone is continuously modified by cloud wind observations. The WO cyclone is treated very realistically by the forecast, hence making the two analyses similar to a high degree.

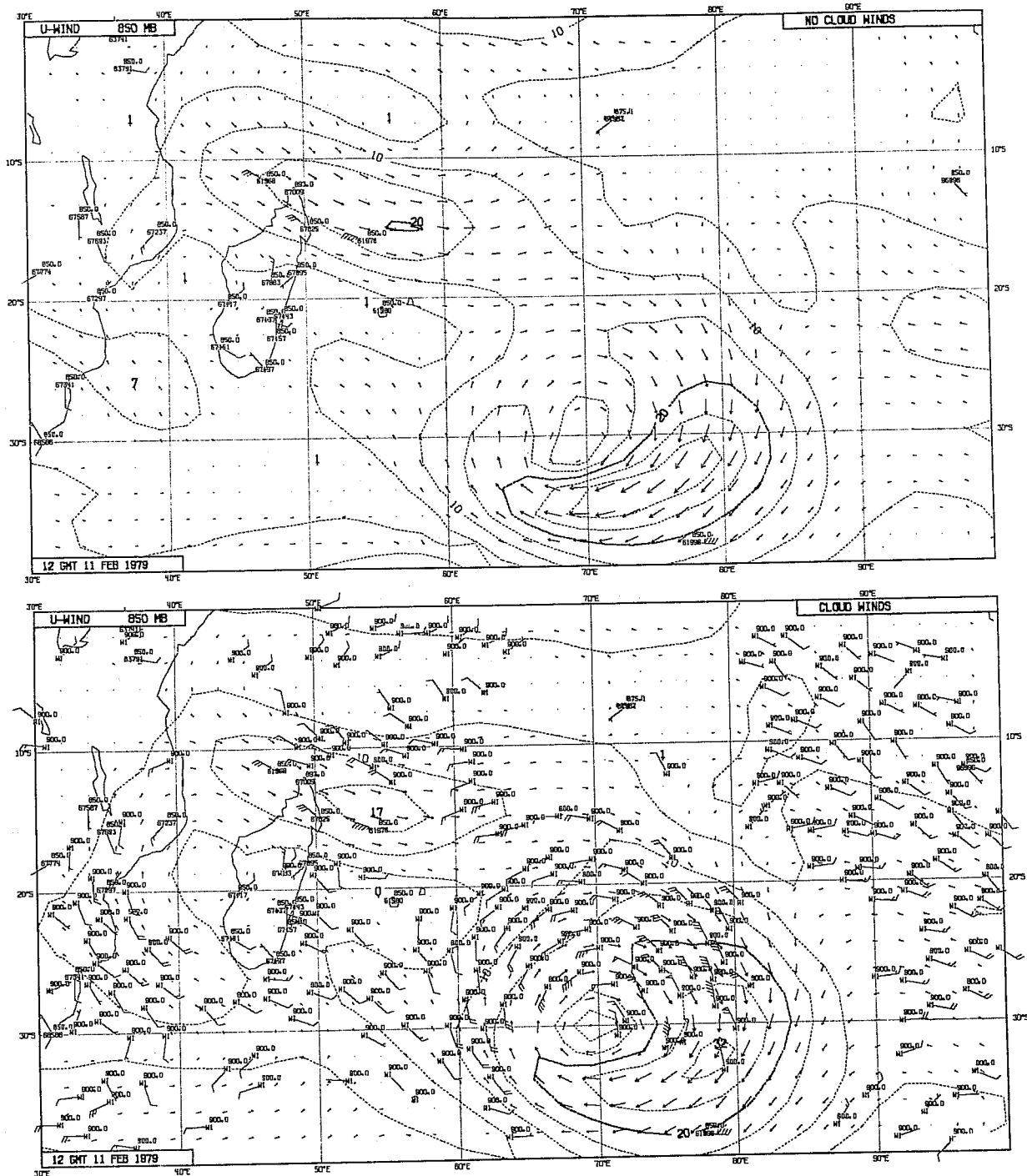


Fig. 17a Wind analysis 850 mb 11 Feb 1979 12 GMT Tropical cyclone "Celine".
No cloudwinds (top), cloudwinds (bottom).

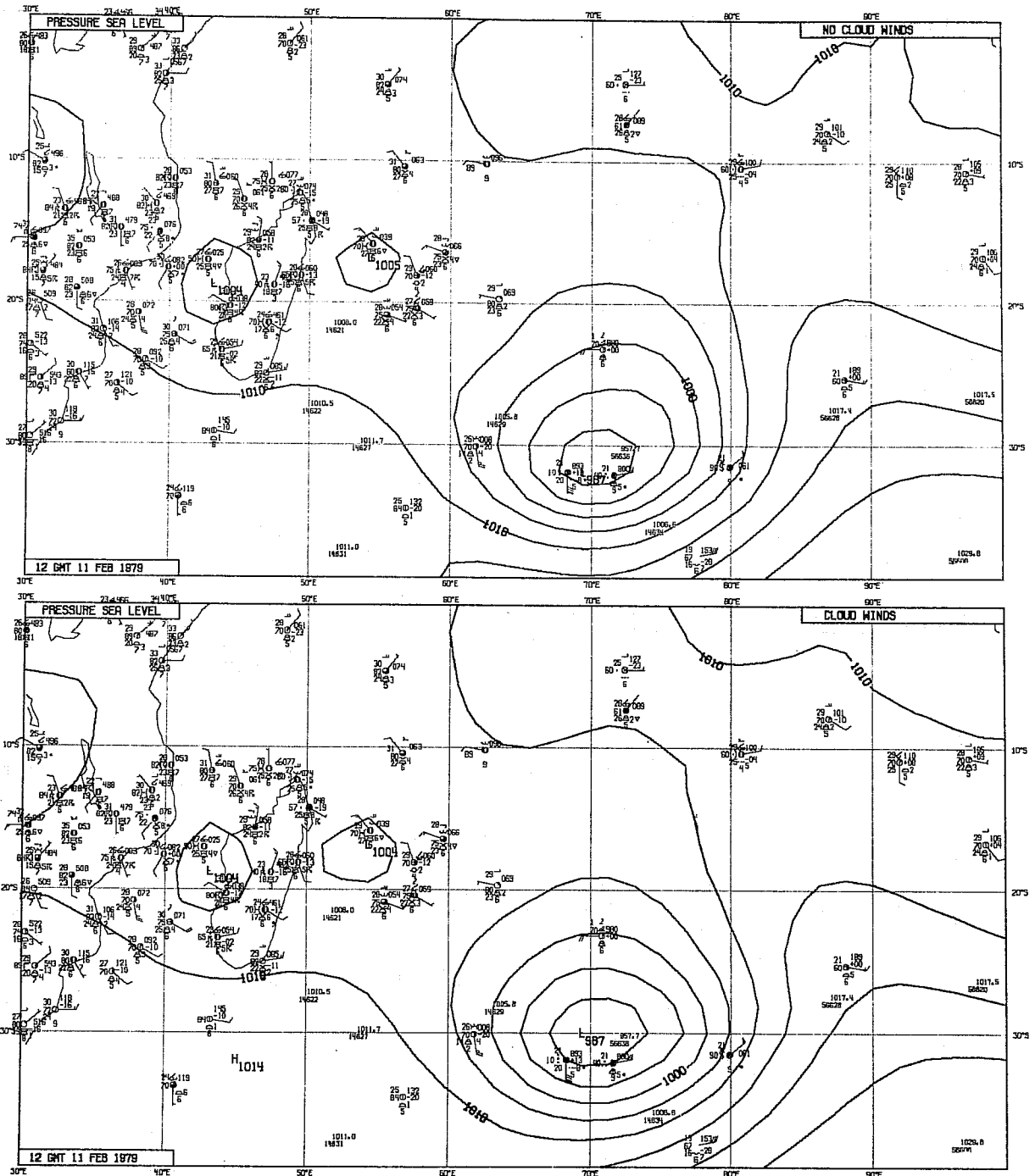


Fig. 17b Mean sea level pressure analysis 11 Feb 1979 12 GMT. No cloudwinds (top), cloudwinds (bottom).

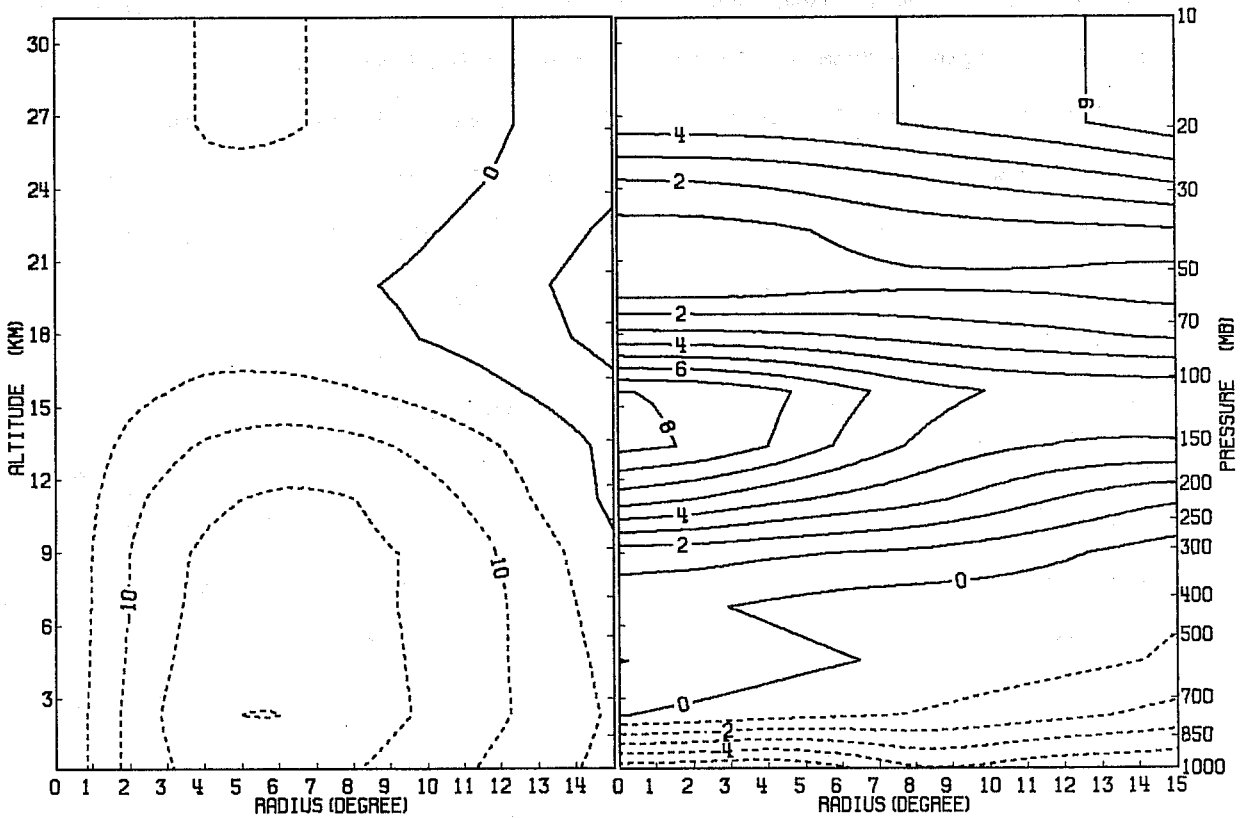
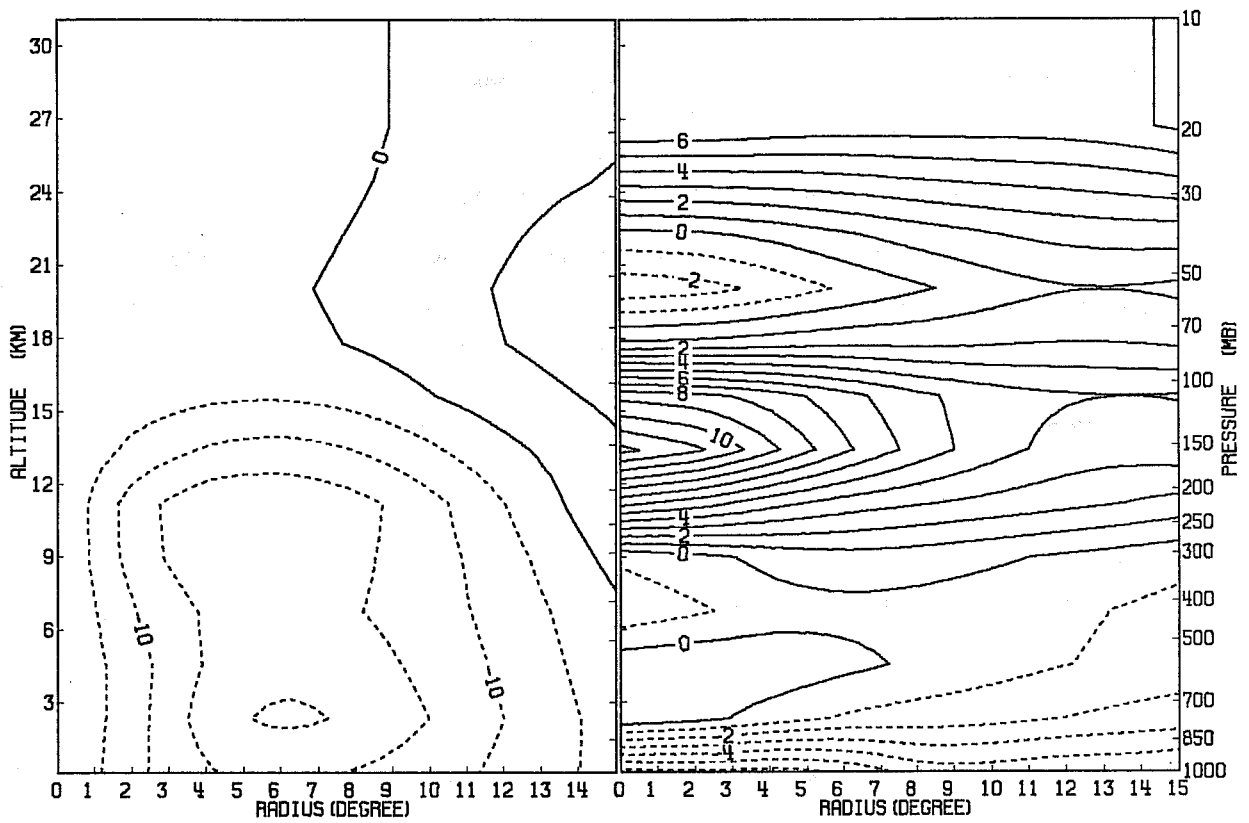


Fig. 18 Thermodynamic structure of tropical cyclone "Celine". No cloudwinds (top), cloudwinds (bottom). Tangential wind, cylindrical average around centre (left). Temperature deviation from area average (right).

4.3 Quality of satellite wind data and problems

in the analysis of these data

Some questions concerning the quality of satellite wind observations and the analysis of these observations arose during the experiment. In this section we will address the following two problems:

- (a) Occurrence of too weak satellite wind reports in the vicinity of the subtropical jet stream.
- (b) Choice of horizontal auto-correlations for tropical wind field analysis.

In several situations during the experiment it was noted that the wind-velocities in the subtropic jet stream in certain areas were much stronger in the WO analyses than in the WI analyses. These differences were found to originate from satellite wind reports which were inconsistent with radiosonde and aircraft reports in their close vicinity. Although these satellite wind reports were associated with larger assumed observational errors than the radiosonde and aircraft reports, their impact still became significant in the WI analyses due to the large number of data. Several examples of suspect wind speeds in satellite wind reports are shown in Fig.19. In this case the analyzed 200 mb wind speed was approximately 10 m/s larger in the WO analysis than in the WI analysis over Sicily and central Italy. It can be seen that cloud drift winds from two different producers, denoted "ME" and "WI" both are much too weak when compared with radiosonde data from Innis (60715), Rome (16242) and Cagliari (16320). In another extreme case the analyzed maximum wind speeds in the subtropical jet stream differed by 30 ms^{-1} between WO and WI. A contributing factor to the acceptance of cloud wind data in preference to radiosonde data in spite of the higher assumed error of the former is the large number of internally consistent satellite winds. The rather high probability of correlated errors

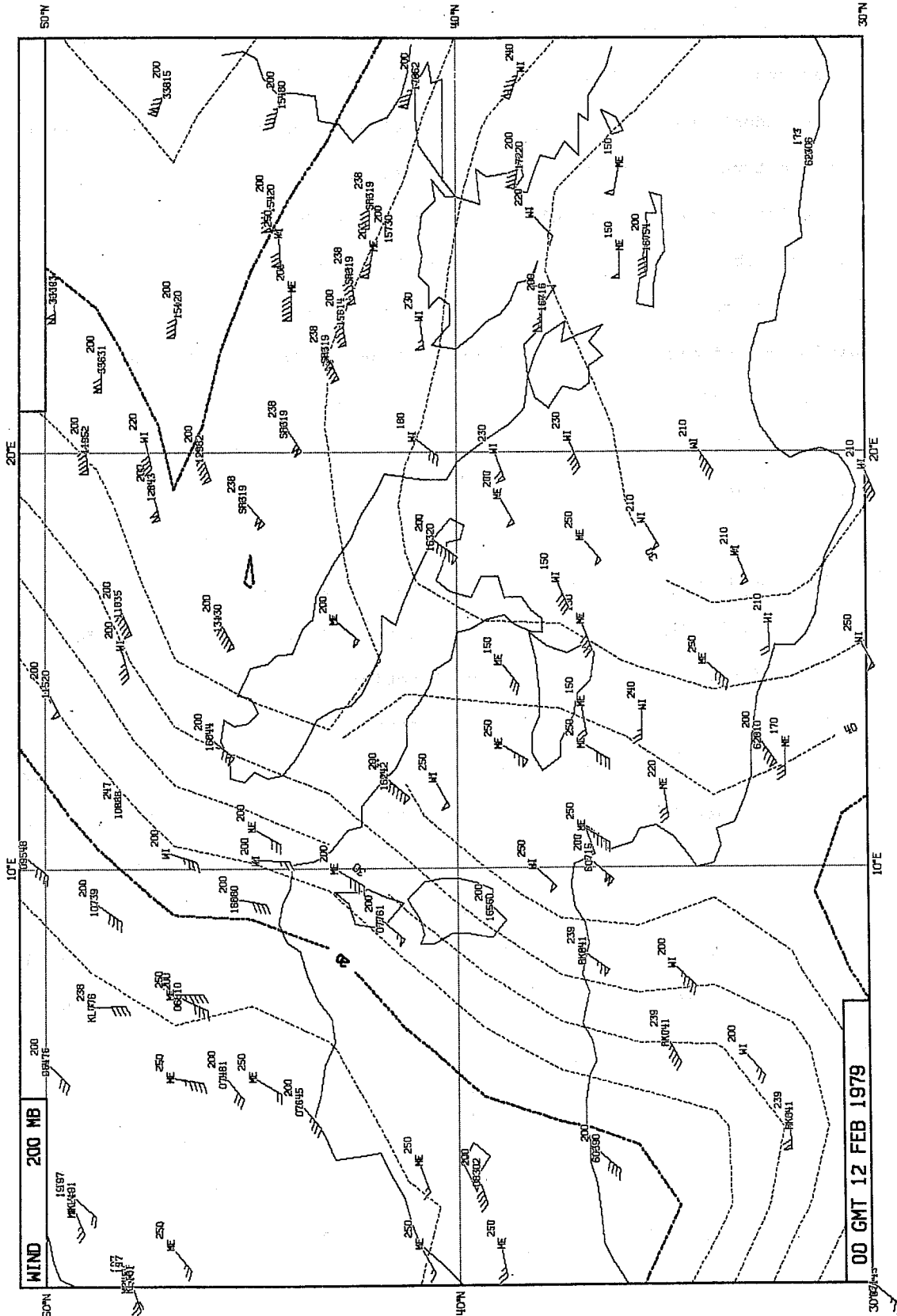


Fig. 19 Analysed isotachs and observed winds Mediterranean. 12 Feb 1979 00 GMT. 5 digit number observations are radiosondes, 2-letter observations are cloud track winds.

in cloud wind observations derived from a local cloud group was not taken into account in the analysis quality checks. The data were instead treated as independent and were confirmed by each other. In order to avoid problems of this nature in the future, cloud wind data should preferably be appended with an indication of local cloud group used for the wind derivation, and a horizontal observation error correlation should be taken into account in the analysis scheme. In this connection it should be pointed out that although rawinsonde and aircraft data positions are uncorrelated to the position of the jet axes, the cloud positions are not necessarily so. Cirrus level clouds may often be found off the jet axis, giving a negative bias to the analysed windspeeds.

The ECMWF optimum interpolation scheme is based on locally non-divergent corrections to a first guess field and for the analysis of the streamfunction a Gaussian isotropic autocorrelation function is utilized. For the wind components this will result in negative correlations at a distance of about 800 km in a direction normal to the wind components. These autocorrelation functions are based on statistics for middle and high latitude numerical forecast errors (Hollett, 1972). They are probably less representative for forecast errors in the tropics. One example of a poor 200 mb wind analysis from the WI assimilation run is given in Fig.20 (12 February 1979 00GMT, detail west of Africa). Some reports from tropical wind observing ships, which were not utilized for the WI analysis, have also been plotted in the figure. Note the large discrepancies between these independent reports and the WI analysis and also note the analysed strong north-easterly flow at 10°N 25°W. This north-easterly flow in the WI analysis developed during several analysis cycles primarily from satellite wind reports in the south-westerly flow at approximately 5°N and 20°W, extrapolated with the autocorrelation functions described above. As a result, the WO analysis was better than the WI analysis in the actual area at 12 February 1979 00GMT. It seems necessary

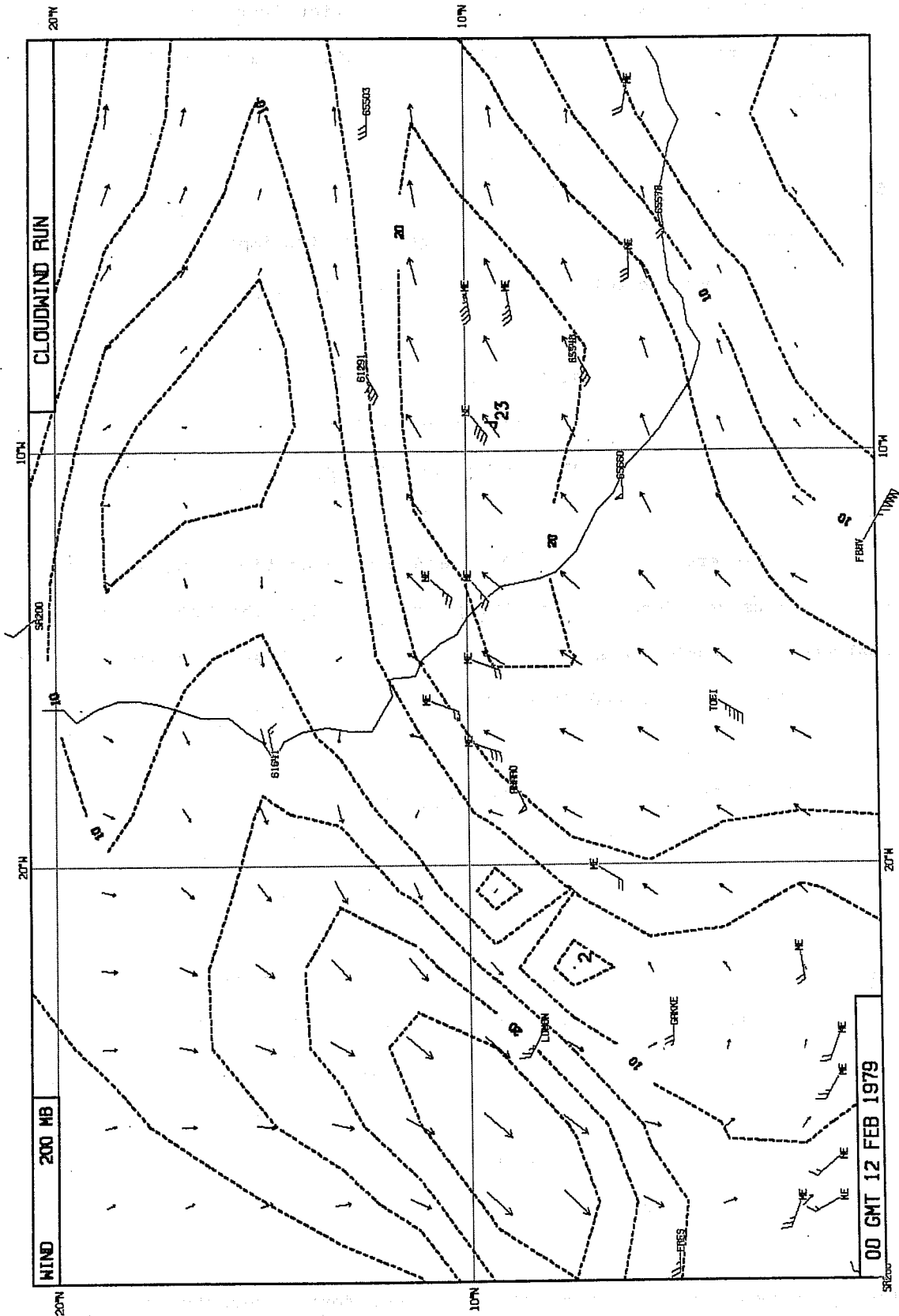


Fig. 20 Analysed and observed winds. West Africa. 12 Feb 00 GMT. TWOS-Ships "LOMON", "GAKKE", "TOFI" and "AMARO" not used for the analysis. Note fictitious NE-flow at 25°W 10°N.

to thoroughly review the choice of autocorrelation functions for the wind analysis and possibly use autocorrelation functions which are dependent on latitude as well as season.

5. IMPACT ON FORECASTS

Four forecast experiments were run to investigate the impact of the satellite wind observations; the following situations were selected.

9 February 1979 12 GMT

12 February 1979 0 GMT

15 February 1979 0 GMT

17 February 1979 12 GMT

All forecasts were run up to 10 days and both synoptical and statistical verifications were done. For the latter verification, the ECMWF Level III-b analyses were considered as the truth since these analyses are based on the most complete observational data set.

5.1 General impact on forecast error statistics

Verification statistics were obtained for several verification areas (see Fig.4). Verification directly against radiosonde observations was also done.

Table 4 contains the averaged values of anomaly correlation for the geopotential height forecasts in the Northern ($20^{\circ}\text{N} - 82.5^{\circ}\text{N}$) and in the Southern ($20^{\circ}\text{S} - 65^{\circ}\text{S}$) hemispheres. The values (in %) are obtained by averaging the standard levels from 1000 to 200 mb and the four cases. The scores are given both for the total fields (wavenumbers 0-20) and for the long waves (1 to 3) separately.

Figure 21 shows the anomaly correlation of the four forecasts individually (for 2-day and 4-day forecasts). If we consider 60% as a measure of useful predictability (Bengtsson, 1981) only the forecasts for days 1 to 6 are

Table 4. Average anomaly correlation 1000-200 mb. Four forecasts.
 WI = with cloudwinds, WO = without cloudwinds.
 Northern Hemisphere (82.5° - 20°N) and Southern
 Hemisphere (82.5°S - 20°S). Wavenumbers 0-20 (total) and
 1-3. Verified against ECMWF III-b.

Forecast range	<u>Northern Hemisphere</u>				<u>Southern Hemisphere</u>			
	Total		Wavenumbers 1-3		Total		Wavenumbers 1-3	
	WI	WO	WI	WO	WI	WO	WI	WO
Day 1	98	98	98	98	93	91	91	88
Day 2	94	94	96	96	85	84	82	79
Day 3	88	87	92	91	79	76	79	73
Day 4	77	76	81	79	71	64	73	63
Day 5	63	61	68	67	59	46	61	43
Day 6	50	49	63	60	51	40	51	33
Day 7	42	42	56	53	44	38	41	23
Day 8	33	32	48	41	37	35	37	22
Day 9	26	22	45	25	25	31	33	23
Day 10	20	14	28	10	15	27	19	20

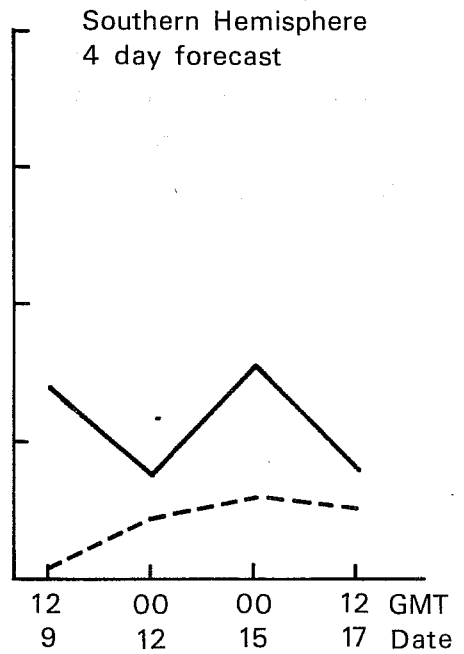
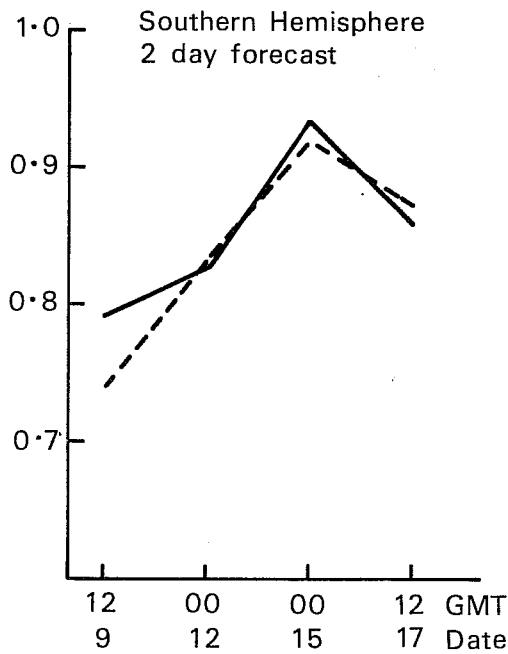
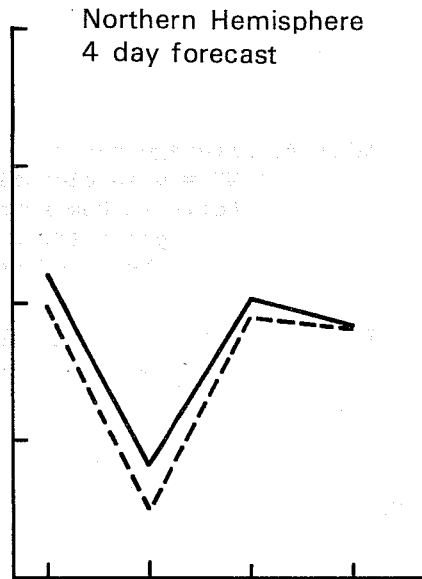
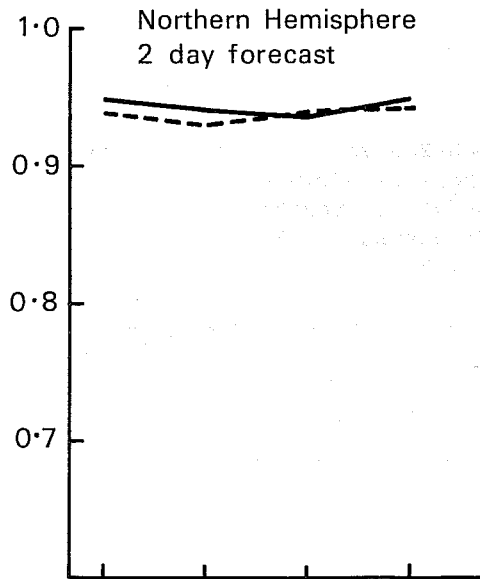


Fig. 21 Anomaly correlation of height 1000-200 mb for mid- and high latitudes of the two hemispheres (20° lat to 82.5° lat). Four forecasts for days 2 and 4. With cloudwinds (full lines), without (dashed).

useful and, for this time range, the scores for the WI forecasts are always better. There is a very significant improvement in predictive skill for the Southern Hemisphere, especially in the long waves. (For the first case (9 February 1979 12GMT) the Southern Hemisphere predictability increases from 4.5 days to 6.5 days when satellite wind data are utilized). For the Northern Hemisphere the improvement is very small according to the verification scores. In both hemispheres the impact is larger for medium-range (4-5 days) forecasts than for short-range (1-3 days) forecasts as can be seen very clearly in Fig.21. The explanation is most likely the clustering of satellite wind observations near the equator and the time it takes for this information to reach higher latitudes.

Due to the great amount of cloud wind observations at high levels, a larger impact can be expected on the 200 mb wind forecasts. Table 5 shows the averaged values of the anomaly correlation for the 200 mb wind forecasts on four different areas (see Fig.4) GL, EQ, SN, SS. The correlations have been averaged for the two wind components and the four cases.

Low latitude circulations are characterized by large scale quasi-stationary systems with superimposed intense subgridscale convection. The performance of global models of the ECMWF type in these areas is very dependent on the subgridscale parameterization scheme used. Also the detrimental effect of the initialization on the initial states in the deep tropics has already been discussed. Thus the predictive skill expressed as anomaly scores, in the tropical regions is generally much more shorter than at higher latitudes. This is reflected in the lower anomaly scores for the low latitude regions in Table 5.

Figure 22 gives the results for the four individual cases (for 1-day and 2-day forecasts), these results have been calculated on the two subtropical

**Table 5 Average anomaly correlation, 200 mb wind forecasts.
Three areas. WI = with cloudwinds, WO = without.**

Forecast range	Global		EQ (15S-15N)		STN (15N-35N)		STS (15S-35S)	
	WI	WO	WI	WO	WI	WO	WI	WO
Day 1	78	72	53	41	85	82	76	69
Day 2	68	63	44	33	77	76	67	55
Day 3	56	53	27	23	69	68	50	41
Day 4	46	43	21	18	56	56	40	33
Day 5	36	33	16	15	52	52	28	26

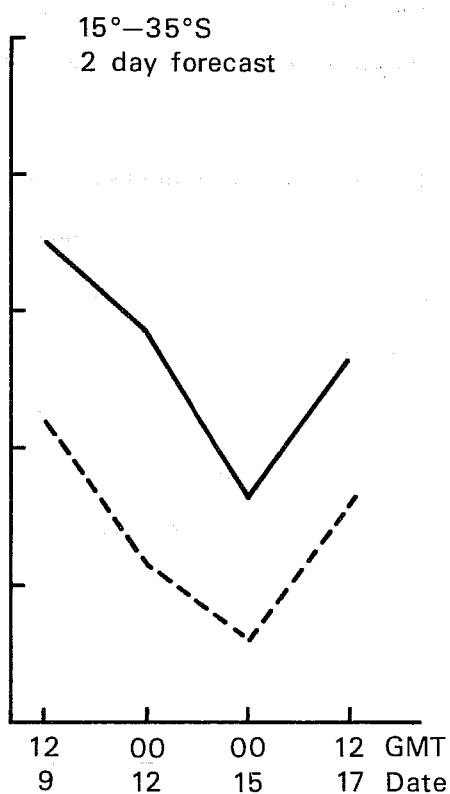
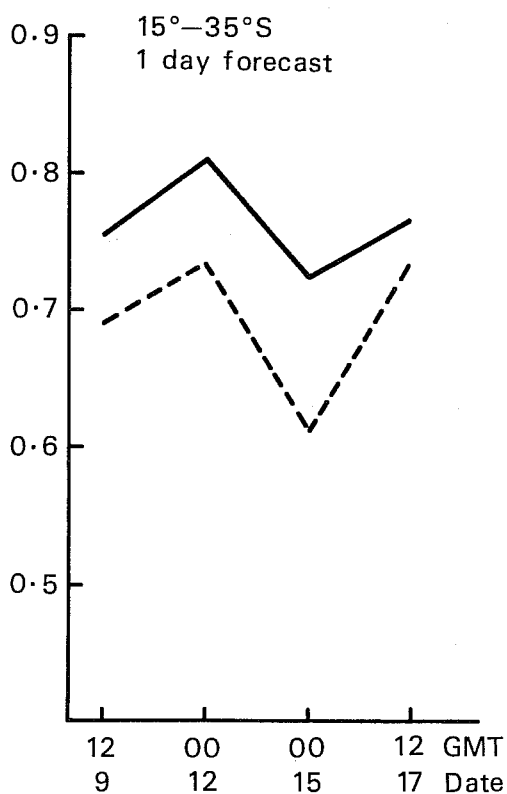
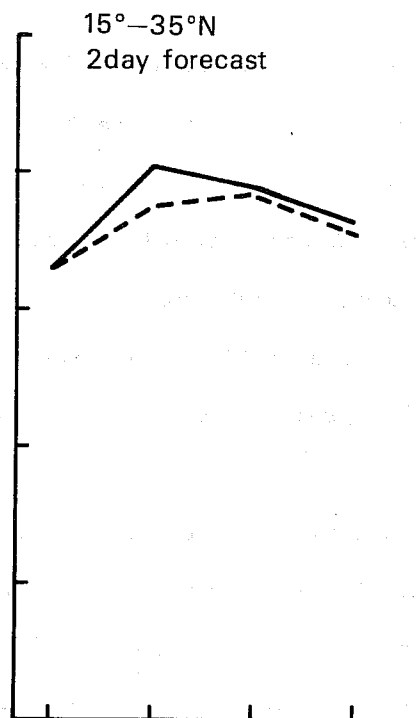
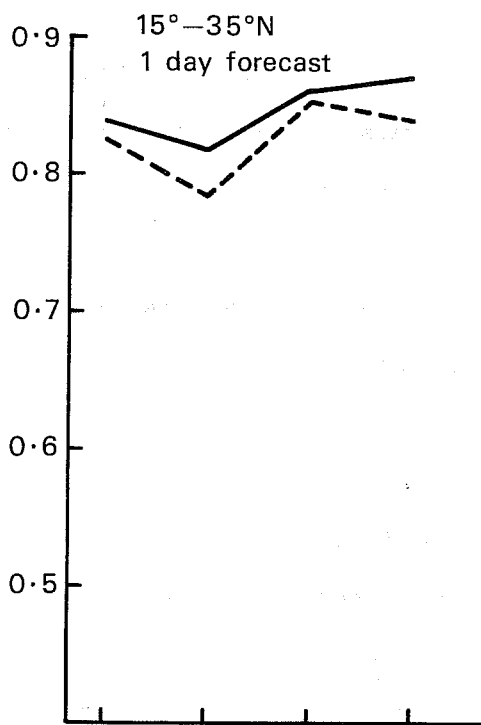


Fig. 22 Anomaly correlations 200 mb wind forecasts. Northern and Southern subtropics (15° lat to 35° lat). Four forecasts for days 1 and 2. With cloudwinds (full lines), without (dashed).

areas. The improvement due to the satellite winds is more marked in these scores than in mass-field scores for the same areas. For the equatorial area the impact is very large, even at day 1, but the forecast quality deteriorates rapidly. The impact is also very large in the Southern Hemisphere subtropical area (15°S - 35°S). It should be remembered, however that the verifying III-b analyses are determined by the cloud wind data for this area to a very high degree.

Statistical evaluation of forecasts against radiosonde observations gives similar results as long as the number of reference observations is large enough. For some cases and for some tropical areas, however, this type of verification does not show the same large positive impact of the satellite wind data as verification against analysed fields. The reason for this is obvious, the WI and WO forecasts mainly differ in areas over the oceans where no radiosonde data are available.

5.2 Synoptic evaluation of forecast maps

For each forecast experiment a synoptic evaluation of the forecast maps was done from day 1 up to day 10. With the exception of a few cases where a detailed investigation was necessary, the evaluation was done for surface and 500 mb mass field maps at middle and high latitudes and 850 and 200 mb wind maps in the tropics. The synoptic evaluation is summarized in Table 6, where the following subjective scores are used.

++ large positive impact of satellite wind observations

+ significant positive impact of satellite wind observations

0 no significant impact of satellite wind observations

- significant negative impact of satellite wind observations

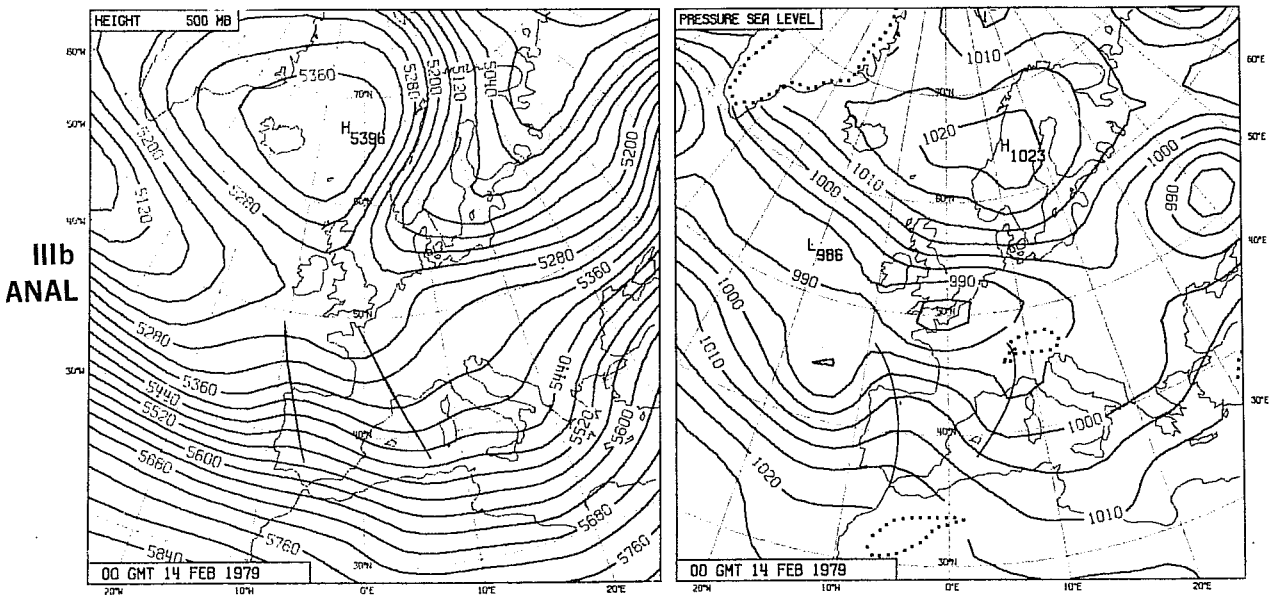
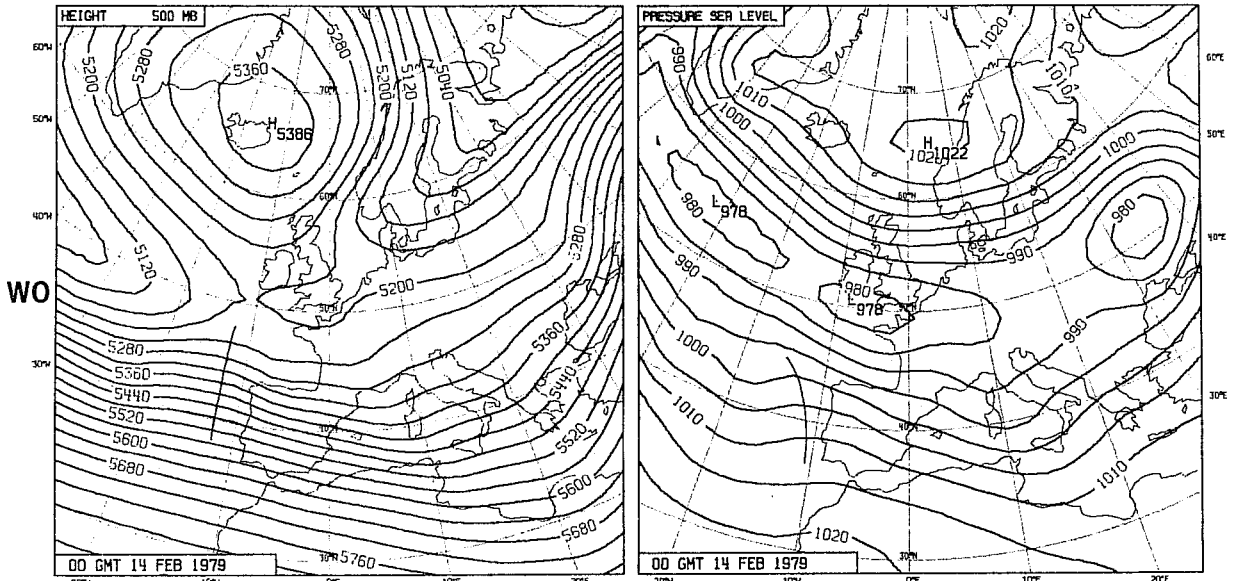
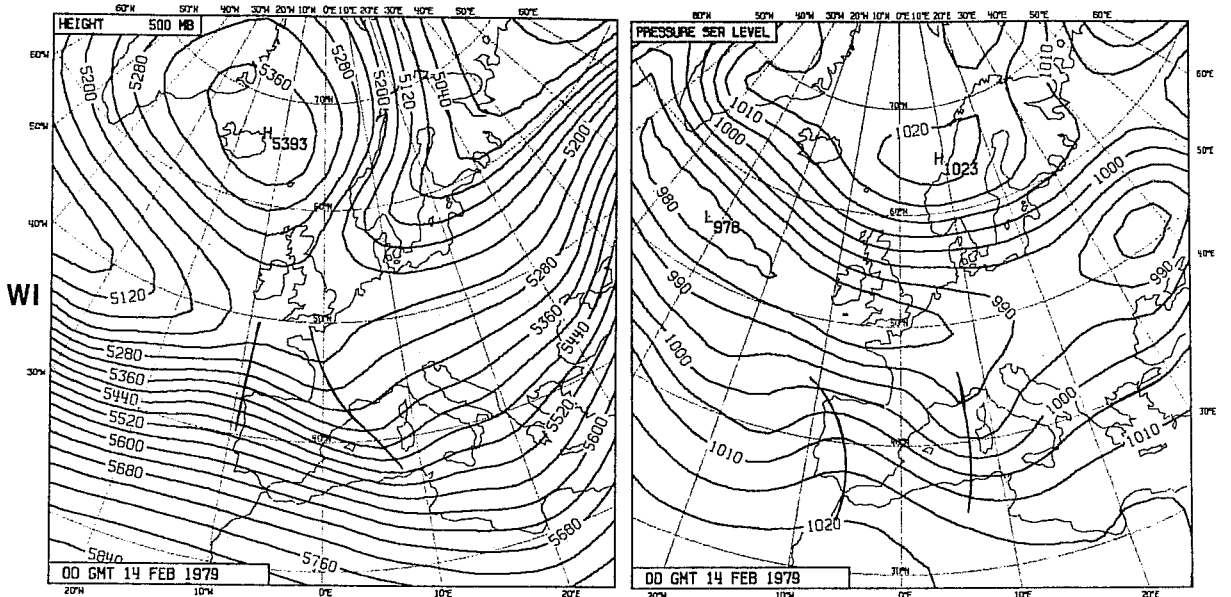
Table 6. Subjective scores for the four forecasts, over three areas.

++ clear positive impact
 + positive impact
 0 no impact
 - negative impact
 -- clear negative impact

	NORTHERN HEMISPHERE					90°N - 30°N
	Forecast length in days					
	1	2	3	4	5	6-10
9.2.79 12GMT	0	0	0	0	0	+
12.2.79 00GMT	0	+	0	0	0	0
15.2.79 00GMT	0	+	+	0	0	0
17.2.79 12GMT	+	-	-	-	-	0

Table	SOUTHERN HEMISPHERE					90°S - 30°S
	Forecast length in days					
	1	2	3	4	5	6-10
9.2.79 12GMT	0	+	++	++	++	+
12.2.70 00GMT	0	+	+	0	0	0
15.2.79 00GMT	+	+	+	++	++	+
17.2.79 00GMT	0	+	+	0	0	0

Table	TROPICS					30°S - 30°N
	Forecast length in days					
	1	2	3	4	5	6-10
9.2.79 00GMT	+	+	+	+	0	0
12.2.79 00GMT	+	++	+	+	0	0
15.2.79 00GMT	+	+	+	0	0	0
17.2.79 00GMT	++	+	+	+	0	0



500mb height

Sea level pressure

Fig. 23 +48 hour forecasts valid 14 Feb 1979 00 GMT with cloudwinds (top) without cloudwinds (middle) and verification (bottom). 500 mb (left) and surface (right).

-- large negative impact of satellite wind observations

In the Northern Hemisphere the impact was never judged to be very large. A small but still significantly positive impact was however found on the maps from the first three forecasts. In the fourth forecast, a negative impact was found. A closer study showed, however, that the negative impact could be traced back to the interaction between humidity analyses and radiation parameterization in the first guess forecasts.

In the Southern Hemisphere there is always a significant positive impact, more pronounced for medium range forecasts (days 3 to 6) than for the short range. The improvement is very marked in 2 cases out of 4 and the subjective evaluation is in close agreement with the statistical evaluation (see the four diagrams of Fig.21). In the tropical belt the improvement from cloud winds is rather large at days 1 and 2, but less so at later times.

Figure 23 shows one of the clearest cases of a positive synoptic impact on the Northern Hemisphere forecasts. They are 2-day forecasts over Europe and the Atlantic ocean from Feb 12th. The wave developing over Portugal, Spain and the Mediterranean Sea is quite well described in the WI forecast while it is much too weak in the WO forecast. Both the ridge over Spain and the trough over the western Mediterranean are better in the WI run. This wave disturbance originated in the central part of the Atlantic ocean where many satellite winds were available for the WI analysis. The predicted fields over western and central Europe are also better in the WI forecast. Over Europe the RMS error of the 500 mb geopotential height forecast is 48 m for the WO run and 33 m for the WI run (a 30% improvement according to this score).

In the first case (9.2.79 12GMT) the WI forecast is much better than the WO forecast over Europe and the Atlantic Ocean for days 6 to 10; an excellent 10-day forecast of the blocking over Europe has been produced by the WI run. Over Europe the RMS of the 10-day forecast for 500 mb geopotential height is 85 m when cloud winds are used, 190 m when they are not used. The quality of this 10-day forecast outside the Atlantic/Europe region is however very bad, and it is not advisable to draw any conclusions on cloud wind impact from the noticed differences.

In summary the results of the synoptic subjective evaluation indicates that the positive impact of cloud winds on forecasts is obvious in the tropics and the Southern Hemisphere, while in the Northern Hemisphere only one case out of four can be considered to show a significant positive impact directly related to the satellite wind data.

6. A FORECAST EXPERIMENT WITH ANALYSES AS LATERAL BOUNDARY

CONDITIONS IN THE TROPICS

The forecast cases described in this report, as well as operational experience at ECMWF, indicate difficulties of the forecast model to predict the circulation in the deep tropics for more than 2 to 3 days. It is very likely that these difficulties reduced the potential impact of tropical cloud wind data on mid latitude medium range forecasts in the present experiments. In order to study this question a bit further, a pair of 10-day forecasts were run, in which the forecast fields were relaxed towards the WI and WO analyses respectively in the deep tropics. This relaxation technique was first suggested by Davies (1976) and is now used by several groups for limited area models. In the tropical band, 30°S - 30°N the forecast gridpoint values are relaxed toward analysed values, using the mixing relation

$$FC^* = \alpha \cdot AN + (1 - \alpha) \cdot FC$$

at each timestep of the forecast. Here FC is the model forecast, AN the analysis which is interpolated linearly between the six hourly analyses and FC* the modified forecast. α is a relaxation coefficient chosen empirically to vary from $\alpha = 1$ at 15° latitude in both hemispheres to $\alpha = 0$ at 30° , in a way that makes the mixing smooth and does not cause reflection in the boundary zone (Kallberg 1977).

Several experiments of this type have been carried out at ECMWF, see Simmons 1981. In the cloud-wind experiment the relaxed forecasts were only marginally better than the full global forecasts from the same initial time. The improvement was slightly larger in the WO case than in the WI case in the Northern Hemisphere. In the Southern Hemisphere no clear improvement was gained from the relaxation in either forecast. The results are inconclusive with regards to the impact of cloud wind data on middle and high latitude forecasts. It is not known whether this is due to inherent weaknesses in the relaxation technique or to inconsistencies in the inserted data. Results from other relaxation experiments do however show a clear improvement on forecasts in some cases (Simmons, 1981) although a great variability from case to case has been found (Haseler, 1982). Very small impact by the tropical forcing may thus indicate a weak coupling between the equatorial circulation and the circulation at higher latitudes in the case used for the present experiment. If this is the case, a larger impact from cloud wind data may be expected in relaxation experiments from other periods. Furthermore, global forecasts may also show larger sensitivity to the presence or absence of tropical cloud wind data for middle and high latitude predictability. For future studies on the possible impact of cloudwind data on medium range forecasts, cases with well defined interaction between low and high latitudes should be selected.

7. SUMMARY AND CONCLUSIONS

Data assimilation experiments with and without satellite wind observations, based on the FGGE data have been carried out for the period 6-19 February 1979, and parallel 10-day numerical forecasts have been run for 4 cases.

The quality of most cloud wind observations was found to be satisfactory, and in most cases the data assimilation system utilized the wind information in a satisfactory way. Some clear weaknesses, both in the cloud wind data themselves and also in the way they were used by the data assimilation, were however identified. They are listed below.

(a) Several cases of high level (cirrus level) wind reports from groups of clouds with far too low windspeeds were encountered. This was the case particularly in the subtropical jetstreams over mountainous regions.

(b) The data assimilation often accepts internally consistent satellite wind reports of poor quality, even when high quality radiosonde and aircraft data are available.

(c) The spatial autocorrelation functions used in the optimum interpolation scheme have been designed for extratropical regions. They sometimes cause less acceptable analyses in the tropics.

(d) Weaknesses in the ability of the ECMWF analysis system to simulate tropical circulation systems have been noticed. These are most likely connected to the parameterization of the physical forcing at low latitudes, and the exclusion of diabatic effects from the initialization.

(e) For data assimilation purposes, the parameterization of physical processes in the forecast model, particularly the radiation-humidity interaction, seems to be too sensitive to small scale noise in the analyses.

Despite these weaknesses, a positive impact of the satellite cloud wind observations, both on the analyses and the forecasts was found. The impact can be summarized as follows.

(a) The wind data have a large positive impact both on the quality of tropical wind analyses and on tropical forecasts for 1 to 3 days. Many synoptic circulation systems are only observed by the cloud drift winds.

(b) The wind data have a large positive impact on numerical forecasts for the Southern Hemisphere. In the four forecast experiments the time range of useful predictability was extended between 1 to 2 days.

(c) In one of the four forecasts, a significant improvement of the northern hemisphere predictability was found.

(d) There was no immediate negative impact from the cloud wind data on any of the forecasts. In one case, the northern hemisphere forecast was slightly worse when the satellite winds had been used. The reason for this was however found to be directly due to the sensitivity of the physical parameterization in the forecast model, and only very indirectly on the different observation subsets used for the analyses.

Based on the results of the experiment it is clear that wind observations from geostationary satellites give a valuable contribution for tropical analyses and short-range forecasts (1-3 days) as well as global medium range forecasts (4-7 days). It must be stressed however, that the results are obtained from the present analysis and forecast systems, which are known to have deficiencies, some of which were highlighted by the experiment.

Results from a forecast experiment where analysed fields replaced the forecast in the deep tropics, indicated that the chosen situation was not characterized by very strong interactions between the tropics and the extratropics. It is likely that the positive impact of cloud drift wind data will be more significant in situations with stronger interaction. Furthermore improvement of the forecast model performance in the deep tropics will also enhance the importance of such data.

ECMWF - GLOBAL FORECASTING SYSTEM, 15-level grid point model

(Horizontal Resolution 1.875° Lat/Lon)

ANALYSIS

PREDICTION

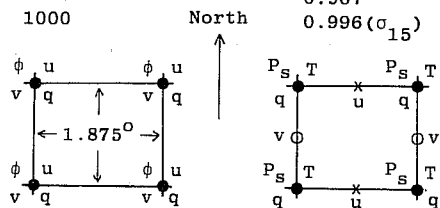
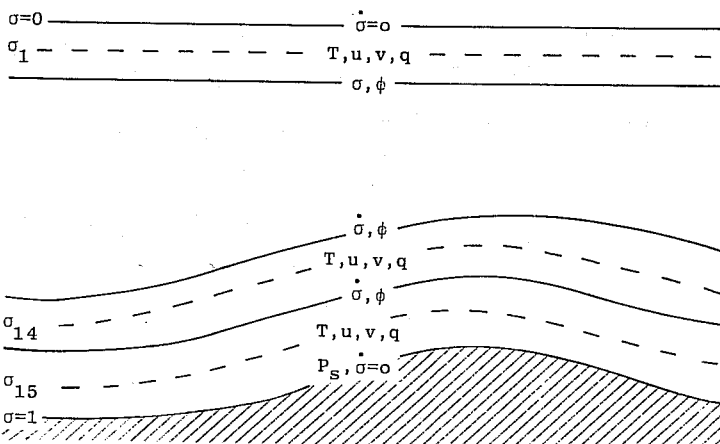
ϕ, u, v, q (for $p > 300$)

T, u, v, q

p (mb)

10
20
30
50
70
100
150
200
250
300
400
500
700
850
1000

σ
0.025 (σ_1)
0.077
0.132
0.193
0.260
0.334
0.415
0.500
0.589
0.678
0.765
0.845
0.914
0.967
0.996 (σ_{15})



Vertical and horizontal (latitude-longitude) grids and dispositions of variables in the analysis (left) and prediction (right) coordinate systems.

ANALYSIS

Method

3 dimensional multi-variate, correction method for q

Independent variables

λ, ϕ, p, t

Dependent variables

ϕ, u, v, q

Grid

Non-staggered, standard pressure levels

First guess

6 hour forecast (complete prediction model)

Data assimilation frequency

6 hour (\pm 3 hour window)

INITIALISATION

Method

Non-linear normal mode, 5 vertical modes, adiabatic

PREDICTION

Independent variables

λ, ϕ, σ, t

Dependent variables

T, u, v, q, p_s

Grid

Staggered in the horizontal (Arakawa C-grid). Uniform horizontal (regular lat/long; $\Delta\lambda = \Delta\theta = 1.875^{\circ}$). Non-uniform vertical spacing of levels (see above).

Finite difference scheme

Second order accuracy

Time-integration

Leapfrog, semi-implicit ($\Delta t = 15$ min) (time filter $\nu = 0.05$)

Horizontal diffusion

Linear, fourth order (diffusion coefficient = $4.5 \cdot 10^{15} \text{ m}^4 \text{ s}^{-1}$)

Earth surface

Albedo, roughness, soil moisture, snow and ice specified geographically. Albedo, soil moisture and snow time dependent.

Orography

Averaged from high resolution (10') data set

Physical parameterisation

- (i) Boundary eddy fluxes dependent on roughness length and local stability (Monin-Obukov)
- (ii) Free-atmosphere turbulent fluxes dependent on mixing length and Richardson number
- (iii) Kuo convection scheme
- (iv) Full interaction between radiation and clouds
- (v) Full hydrological cycle
- (vi) Computed land temperature, no diurnal cycle
- (vii) Climatological sea-surface temperature

Appendix 1

References

- Bengtsson, L., M.Kanamitsu, P.Kallberg, S.Uppala 1982 FGGE 4-Dimensional Data Assimilation at ECMWF. Bull.Am.Met.Soc., 63, No.1 January 1982.
- Hollett, S.R. 1975 Three dimensional spatial correlations of PE forecast errors. MS thesis. Dept. of Meteorology, McGill University, Montreal.
- Lorenc, A., 1981 A global three-dimensional multivariate statistical interpolation scheme Mon.Wea.Rev., 109, 701-721.
- Schlatter, T. 1981 An assessment of operational TIROS-N temperature retrievals over the U.S. Mon.Wea.Rev., 109, 110-119.
- Newell, R.E., J.W.Kidson, G.D.Vincent and G.J.Boer 1972 The General Circulation of the Tropical Atmosphere and Interactions with Extratropical Latitudes. Vol.1 The MIT Press, Cambridge, Mass. and London. 258 pp.
- Krishnamurty, T.N. 1979 Large-scale features of the Tropical Atmosphere. Meteorology over the Tropical Oceans, pp.31-56. Roy.Met.Soc.
- Davies, H.C. 1976 A lateral boundary formulation for multi-level prediction models. Quart.J.R.Met.Soc. 102, pp.405-418.
- Simmons, A. 1981 Tropical Influences on Stationary Wave Motion in Middle and High Latitudes. ECMWF Tech.Rep.No.26.
- Haseler, J. 1982 ECMWF Tech.Rep. (to be published).
- Kallberg, P. 1977 Test of a Lateral Boundary Relaxation Scheme in a Barotropic Model. ECMWF Internal Report No.3.

ECMWF PUBLISHED TECHNICAL REPORTS

- No. 1 A Case Study of a Ten Day Prediction
- No. 2 The Effect of Arithmetic Precisions on some Meteorological Integrations
- No. 3 Mixed-Radix Fast Fourier Transforms without Reordering
- No. 4 A Model for Medium-Range Weather Forecasting - Adiabatic Formulation
- No. 5 A Study of some Parameterizations of Sub-Grid Processes in a Baroclinic Wave in a Two-Dimensional Model
- No. 6 The ECMWF Analysis and Data Assimilation Scheme - Analysis of Mass and Wind Fields
- No. 7 A Ten Day High Resolution Non-Adiabatic Spectral Integration: A Comparative Study
- No. 8 On the Asymptotic Behaviour of Simple Stochastic-Dynamic Systems
- No. 9 On Balance Requirements as Initial Conditions
- No.10 ECMWF Model - Parameterization of Sub-Grid Processes
- No.11 Normal Mode Initialization for a multi-level Gridpoint Model
- No.12 Data Assimilation Experiments
- No.13 Comparison of Medium Range Forecasts made with two Parameterization Schemes
- No.14 On Initial Conditions for Non-Hydrostatic Models
- No.15 Adiabatic Formulation and Organization of ECMWF's Spectral Model
- No.16 Model Studies of a Developing Boundary Layer over the Ocean
- No.17 The Response of a Global Barotropic Model to Forcing by Large-Scale Orography
- No.18 Confidence Limits for Verification and Energetics Studies
- No.19 A Low Order Barotropic Model on the Sphere with the Orographic and Newtonian Forcing
- No.20 A Review of the Normal Mode Initialization Method
- No.21 The Adjoint Equation Technique Applied to Meteorological Problems
- No.22 The Use of Empirical Methods for Mesoscale Pressure Forecasts
- No.23 Comparison of Medium Range Forecasts made with Models using Spectral or Finite Difference Techniques in the Horizontal
- No.24 On the Average Errors of an Ensemble of Forecasts
- No.25 On the Atmospheric Factors Affecting the Levantine Sea
- No.26 Tropical Influences on Stationary Wave Motion in Middle and High Latitudes

ECMWF PUBLISHED TECHNICAL REPORTS

- No.27 The Energy Budgets in North America, North Atlantic and Europe Based on ECMWF Analyses and Forecasts
- No.28 An Energy and Angular-Momentum Conserving Vertical Finite-Difference Scheme, Hybrid Coordinates, and Medium-Range Weather Prediction
- No.29 Orographic Influences on Mediterranean Lee Cyclogenesis and European Blocking in a Global Numerical Model
- No.30 Review and Re-assessment of ECNET - a private network with Open Architecture
- No.31 An Investigation of the Impact at Middle and High Latitudes of Tropical Forecast Errors
- No.32 Short and Medium Range Forecast Differences Between a Spectral and Grid Point Model. An Extensive Quasi-Operational Comparison
- No.33 Numerical Simulations of a Case of Blocking: The Effects of Orography and Land-Sea Contrast
- No.34 The Impact of Cloud Track Wind Data on Global Analyses and Medium Range Forecasts